University of Brasilia at Gama – FGA/UnB
Biomedical Engineering Graduate Program

Dynamical systems approach to theoretical models of diseases: Application to nonlinear HIV dynamics and blood vessel flows with aneurysm

Lorena de Sousa Moreira

Advisor: Dr. Ronni Geraldo Gomes de Amorim
Coadvisor: Dr. Rodrigo Andrés Miranda Cerda

UNIVERSITY OF BRASILIA AT GAMA

Programa de
Pós-Graduação em
ENGENHARIA BIOMÉDICA

DYNAMICAL SYSTEMS APPROACH TO THEORETICAL MODELS OF DISEASES: APPLICATION TO NONLINEAR HIV DYNAMICS AND BLOOD VESSEL FLOWS WITH ANEURYSM

LORENA DE SOUSA MOREIRA

ADVISOR: RONNI GERALDO GOMES DE AMORIM

COADVISOR: RODRIGO ANDRÉS MIRANDA CERDA

MASTER DEGREE THESIS ON
BIOMEDICAL ENGINEERING

PUBLICATION: 116A/2020

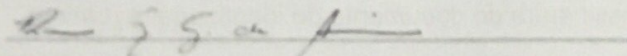BRASILIA/DF, FEBRUARY 2020

UNIVERSITY OF BRASILIA AT GAMA

GRADUATE PROGRAM

DYNAMICAL SYSTEMS APPROACH TO THEORETICAL MODELS OF DISEASES: APPLICATION TO NONLINEAR HIV DYNAMICS AND BLOOD VESSEL FLOWS WITH ANEURYSM
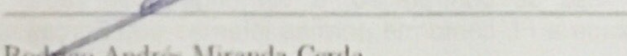
LORENA DE SOUSA MOREIRA

MASTER THESIS SUBMITTED TO THE BIOMEDICAL ENGINEERING GRADUATE PROGRAM, AS A PARTIAL FULFILLMENT OF THE REQUIREMENTS FOR THE DEGREE OF MASTER IN BIOMEDICAL ENGINEERING
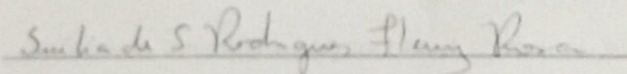
APPROVED BY:

_____

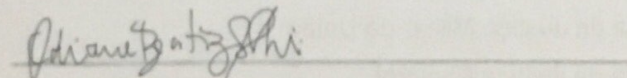Ronni Geraldo Gomes de Amorim

(Advisor)

_____

Rodrigo Andrés Miranda Cerda

(Coadvisor)

_____

Dr. Suélia de Siqueira Rodrigues Fleury Rosa

(Internal examiner)

_____

Dr. Adriane Beatriz Schelin

(External examiner)

Catalog Card

> Moreira, Lorena de Sousa
>
> Dynamical systems approach to theoretical models of diseases: Application to nonlinear HIV dynamics and blood vessel flows with aneurysm [Distrito Federal], 2020.
>
> 40p., 210 × 297 mm (FGA/UnB Gama, Mestrado em Engenharia Biomédica, 2020).
>
> Dissertação de Mestrado em Engenharia Biomédica, Faculdade UnB Gama, Programa de Pós-Graduação em Engenharia Biomédica.
>
> | | |
> |---|---|
> | 1. Nonlinear Dynamics | 2. Chaos |
> | 3. Numerical Simulation | 4. Bifurcation |
> | 5. Intermittency | 6. Coherent Structures |
> | I. FGA UnB/UnB. | II. Título (Série). |

Reference

Copyright

Autor: Lorena de Sousa Moreira

Título: Dynamical systems approach to theoretical models of diseases: Application to nonlinear HIV dynamics and blood vessel flows with aneurysm

Grau: Mestre

Ano: 2020

moreira.lorena@ymail.com

Brasília, DF – Brasil

"Upset the established order and everything becomes chaos.
I'm an agent of chaos, and you know the thing about chaos..."
Joker

I dedicate this work and all my conquests to my beloved parents, Almiro and Lindalva, and my sister, Luana, who are always supporting me.

Acknowledgments

First and foremost I would like to thank my coadvisor, Rodrigo Miranda, for his guidance and support over the past few years. I've benefited from patient advice and learned an incredible amount working with him.

Second, I would like to thank Ronni Amorim for guidance and for pushing me to be precise have shaped how I think about physics.

I'd further like to thank Leandro Xavier for valuable contributions in the Qualification Exam. I'd also like to thank the members of my master thesis committee: Adriane Schelin and Suélia Rosa. All three have a broad and rich knowledge of physics and engineering and I'm lucky to have had the opportunity to interact with them.

I'd like to thank FAPDF for the financial support for my presentation of this work as an oral presentation to the VIII Latin American Conference on Biomedical Engineering and XLII National Conference on Biomedical Engineering, held in Cancún, Mexico.

Resumo Estendido

Abordagem de sistemas dinâmicos para modelos teóricos de doenças: aplicação à dinâmica não-linear do HIV e fluxos de vasos sanguíneos com aneurisma

Lorena de Sousa Moreira

Palavras-chave: Dinâmica Não-linear; Caos; Simulação Numérica; Bifurcação; Intermitência; Estruturas Coerentes.

1 Introdução

Modelos teóricos podem fornecer meios confiáveis para viabilizar previsões sobre a interação do HIV com as células imunitárias, o surgimento de infecções oportunistas, a efetividade medicamentosa; além de descrever a dinâmica de fluxos sanguíneos na presença de doenças circulatórias, tais como, aneurisma e estenose.

O comportamento da população viral pode ser controlado através de tratamentos. Por outro lado, infecções oportunistas podem trazer complicações e afetar o comportamento do vírus.

A presença de estruturas coerentes pode influenciar na circulação de células no sangue, assim contribuindo para o acúmulo dessas e formação de barreiras nos vasos sanguíneos.

Neste trabalho foi realizado uma análise do caos em sistemas biomédicos a partir de simulação numérica de modelos teóricos não-lineares.

Um dos modelos numéricos utilizado para o estudo foi um modelo simplificado modificado da dinâmica do HIV, com o surgimento de infecções oportunistas, e incluído dois tratamentos antirretrovirais. Também foi realizada análise da terapia antirretroviral por meio do estudo de sua efetividade.

O outro modelo não-linear estudado é em relação ao comportamento do fluxo sanguíneo nos vasos que tem a presença de aneurisma. A partir da simulação numérica pode ser realizado uma análise do escoamento de fluido e a identificação de estruturas coerentes.

O objetivo principal deste trabalho é apresentar uma análise desses modelos não-lineares simplificados, aplicando ferramentas de sistemas não-lineares.

O estudo pretende também avaliar o comportamento matemático do HIV ao infectar as células do sistema imunológico e o desenvolvimento de infecções oportunistas; avaliar a efetividade de dois tipos de tratamentos antirretrovirais; demonstrar a transição da dinâmica ordenada à caótica conforme há variações de eficácia do tratamento antirretroviral; simular numericamente o comportamento do fluxo de sangue em um modelo simplificado de vaso sanguíneo com presença de aneurisma; caracterizar a influência da amplitude do aneurisma na geração de estruturas coerentes, que são responsáveis pela alteração da circulação de partículas no sangue.

2 Caos

Uma das descobertas matemáticas notáveis do século XX foi que sistemas simples podem apresentar comportamento imprevisível. O motivo desse comportamento imprevisível foi intitulado "caos" [6]. O efeito do caos é a sensibilidade.

Os efeitos essenciais para a Teoria do Caos estão relacionados à sensibilidade às condições iniciais e à previsibilidade limitada. A Teoria do Caos é um instrumento que auxilia a análise de sistemas dinâmicos não-lineares. Esses sistemas não-lineares exibem um comportamento aleatório [9].

A Teoria de Caos é aplicada aos dois cenários propostos, tanto para o modelo simplicado modificado do comportamento do HIV quanto ao modelo simplificado do vaso sanguíneo com aneurisma. Além dos modelos propostos, a Teoria de Caos é aplicada em diferentes áreas, como nas bolsas de valores, meteorologia e oceanografia.

3 Vírus da Imunodeficiência Humana

A infecção causada pelo HIV prejudica os glóbulos brancos, também conhecidos como leucócitos, que são os responsáveis pela imunidade mediada pelos antígenos. O HIV tem como alvo principal os linfócitos T auxiliares, representados também como linfócitos T CD4$^+$. Os linfócitos T CD4$^+$ são responsáveis por coordenar a função do sistema de defesa imunológica contra, principalmente, vírus, bactérias e fungos [1] [4].

As estatísticas globais divulgadas pelo Programa Conjunto das Nações Unidas sobre HIV/AIDS [12] estimaram que em 2017 cerca de 36,9 milhões de pessoas estão vivendo com HIV em todo o mundo. Com base nessas estatísticas, é necessário estudar mais a progressão da doença, bem como o tratamento mais eficaz e as doenças oportunistas que possam surgir.

Ainda não há tratamento disponível que seja capaz de eliminar o HIV do organismo humano. Contudo, há tratamentos que visam retardar a velocidade do processo prejudicial causado ao sistema imunológico. Medicamentos que atuam como inibidores de transcriptase reversa e os inibidores de protease são exemplos de terapias antirretrovirais [12].

Os inibidores de transcriptase reversa atuam na enzima de transcriptase reversa im-

pedindo que ocorra a infecção de células, impossibilitando que o RNA do vírus HIV se transforme em DNA complementar. Os inibidores de protease bloqueiam a fragmentação da enzima protease do precursor viral, impedindo a maturação do vírus [1].

Há análises de modelos teóricos não-lineares que estudam a relação entre o HIV e o sistema imunológico, a evolução da infecção por HIV associada ao surgimento de doenças oportunistas. Esses estudos numéricos podem ser observados em Anderson e May [2], Li e Wang [7], Lund et al. [8], Perelson et al. [10], Wang [13].

O presente trabalho é composto por um modelo simplificado modificado da dinâmica do HIV na presença de uma infecção oportunista, que descreve a dinâmica não-linear da população de linfócitos T CD4$^+$ e sua interação com o HIV, assim como a inclusão de dois tipos de tratamento antirretroviral.

O tratamento antirretroviral é representado por dois parâmetros, σ_1 e σ_2, que representam os inibidores da transcriptase reversa e o inibidor de protease, respectivamente.

O modelo é descrito pelo seguinte conjunto de Equações Diferenciais Ordinárias

$$
\begin{aligned}
\dot{P} &= \Lambda - \mu P - \gamma PV, & (1) \\
\dot{X} &= \gamma PV + rX - \beta XV - dX^2 + kIX, & (2) \\
\dot{Y} &= \sigma_1 \beta XV - \alpha Y, & (3) \\
\dot{V} &= \sigma_2 \lambda \alpha Y - bV - \delta(X + Y)V - \sigma XV, & (4) \\
\dot{I} &= cI - hIX, & (5)
\end{aligned}
$$

As equações (3.1)-(3.5) são obtidas descrevendo a interação entre células T CD4$^+$ e vírus HIV usando um modelo não-linear de predador-presa. Esses modelos podem reproduzir com sucesso várias características observadas em pacientes infectados, como longos períodos transitórios de latência, depleção de células T saudáveis e o aumento exponencial das taxas de vírus HIV e de infecções oportunistas [2][8][10].

4 Simulação Numérica de Fluxos Sanguíneos

Há modelos teóricos que envolvem fenômenos hemodinâmicos. Esses estudos são de grande importância em virtude das limitações relevantes de análises *in vitro* e da incapacidade de replicação dos vasos sanguíneos humano em modelos animais.

A simulação computacional é uma técnica que permite a execução da análise hemodinâmica de maneira viável, barata e rápida. Além de permitir que a estrutura anatômica dos vasos sanguíneos seja reproduzida, pois se utiliza códigos numéricos para a previsão do comportamento do fluxo sanguíneo seja qual for à circunstância.

Portanto, a simulação computacional permite a análise numérica do escoamento de fluidos. Através dela é possível realizar intervenções virtuais com o propósito de auxiliar diagnóstico e tratamento.

O escoamento de fluidos pode apresentar comportamentos diferentes dependendo das características do fluido e das dimensões do canal, existindo diversas classificações tais como laminar, periódico ou turbulento. Além disso, partículas submersas no fluido podem seguir trajetórias caóticas, mesmo na presença de um fluido laminar [5].

Fluxos sanguíneos turbulentos podem gerar estruturas filamentares que catalisam a atividade de partículas reagentes, e que podem levar à aceleração de processos bioquímicos, fazendo com que determinadas partículas, como plaquetas, tenham mais facilidade em se aglomerar [11].

A detecção de estruturas filamentares em fluidos turbulentos é tema de grande interesse na comunidade científica. Diversas técnicas foram propostas para separar as flutuações randômicas das estruturas coerentes persistentes. Diversas doenças circulatórias podem interferir na formação de estruturas coerentes e no comportamento do fluxo sanguíneo, como o aneurisma [3].

Este trabalho simulou numericamente um modelo simplificado de um vaso sanguíneo na presença de um aneurisma. Para realizar a simulação, este modelo simplificado foi elaborado usando o software Comsol Multiphysics.

Primeiramente, foram selecionados os tempos de 0 e 1.25 segundos como retratos do fluxo sanguíneo, e selecionadas as amplitudes do aneurisma foram selecionadas 0,2, 0,6, 1,0 e 1,4 cm. Foi realizada a análise do fluxo sanguíneo para cada amplitude do aneurisma selecionado. Depois foi realizada uma análise de cada amplitude selecionada, referente ao expoente de Lyapunov para tempo finito. O intervalo de tempo determinado foi 0.625 segundos e 1.25 segundos, para poder realizar uma comparação com a análise inicial, seguindo a estrutura adotada para a execução do software Comsol Multiphysics.

As variações no tamanho do aneurisma no vaso permitiram avaliar as mudanças que ocorrem no comportamento dos fluidos. Também pode ser identificado que a amplitude do aneurisma interfere no aumento de formação de estruturas coerentes.

A formação de estruturas coerentes pode acarretar em prejuízos à saúde. Essas estruturas podem diminuir o tempo de duração de processos bioquímicos, modificando o comportamento de partículas presentes no sangue. Essas partículas podem se aglomerar, como nos casos de plaquetas, podendo formar trombos; ou no caso de partículas de gordura, formando ateromas. As estruturas coerentes também podem influenciar no caso de partículas de princípios ativos de medicamentos, pois se uma partícula ficar retida em determinada região, esta não se ligará ao seu receptor, assim, diminuindo a eficácia medicamentosa.

5 Conclusão

Como conclusão deste trabalho verificou-se que ao diminuir a eficiência do tratamento há transição da dinâmica regular para a caótica através de uma cascata de duplicação periódica, ocasionando em regime caótico. A dinâmica caótica do HIV pode exibir comportamento intermitente, no qual a dinâmica regular é interrompida por estouros caóticos. A dinâmica regular mostra o comportamento da efetividade da terapia antirretroviral. Os resultados obtidos podem contribuir para compreender a dinâmica do HIV e prever surtos irregulares do vírus, tal como o aparecimento de infecção oportunistas.

Os resultados apresentados para a simulação numérica do fluxo sanguíneo possibilitam observar que a amplitude do aneurisma interfere na formação de estruturas coerentes. Foi possível determinar e analisar as estruturas coerentes através da delimitação de contorno dessas estruturas. É possível observar a formação de vórtice no modelo. O fluido gera um vórtice no início do vaso e com o passar do tempo esse vórtice se dissipa. Então há a formação de outro vórtice, novamente na região inicial do vaso.

As outras estruturas evidentemente formadas são linhas bem definidas, criando barreiras de transporte. As barreiras de transporte podem influenciar na aglomeração de partículas e formação de coágulos. A localização da formação de estruturas coerentes pode influenciar no enfraquecimento da parede do vaso, pois provocam uma pressão e tensão em determinado ponto da parede ao desviar parte o fluxo sanguíneo. Esse acúmulo de fluxo em uma região pode influenciar no rompimento do aneurisma, forma mais grave da patologia, podendo ocasionar em morte. A análise sobre esse modelo requer estudos mais detalhados, através das alterações dos parâmetros das equações do modelo.

Lista de Referências

[1] A. K. Abbas, A. H. Lichtman, e S. Pillai. *Imunologia Celular e Molecular.* Elsevier Editora Ltda., Rio de Janeiro, RJ, 9ª edição, 2019.

[2] R. M. Anderson e R. M. May. *Complex dynamical behavior in the interaction between HIV and the immune system. In Cell to Cell Signalling: From Experiments to Theoretical Models.* Academic Press, Belgium, 1989.

[3] B. M. C. Azevedo. *Estudo preliminar da hemodinâmica em modelos simplificados de aneurismas saculares.* Dissertação de mestrado, Mestrado Integrado em Engenharia Mecânica, Faculdade de Engenharia da Universidade do Porto, 2010.

[4] E. R. Cachay. *Infecção pelo vírus da imunodeficiência humana (HIV). Manual MSD: versão para profissionais de saúde. Merck Sharp & Dohme Corp, New Jersey, 2018.*

[5] P. A. Davidson. *Turbulence: an introduction for scientists and engineers.* Oxford Univ. Press., New York, 1ª edição, 2004.

[6] R. A. Devaney. *A First Course In Chaotic Dynamical Systems: Theory And Experiment.* Avalon Publishing, New York, 1ª edição, 1992.

[7] M. Y. Li e L. Wang. Backward bifurcation in a mathematical model for HIV infection in vivo with anti-retroviral treatment. *Nonlinear Analysis Real World Applications*, 17(1):147–160, 2014.

[8] O. Lund, E. Mosekilde, e J. Hansen. Periodic doubling route to chaos in a model of HIV infection of the immune system. *Simulation Practice and Theory*, 1(2):49–55, November 1993.

[9] R. A. Miranda. *Simulação numérica da interação onda-onda induzida por onda de Langmuir no sistema solar.* Dissertação de mestrado, Mestrado em Geofísica Espacial, Instituto Nacional de Pesquisas Espaciais, 2006.

[10] A. S. Perelson, D. E. Kirschner, e R. de Boer. Dynamics of HIV infection of CD4+ T cells. *Mathematical Biosciences*, 114(1):81–125, 1993.

[11] A. B. Schelin, Gy. Károlyi, A. P. S. de Moura, N. A. Booth, e C. Grebogi. Chaotic advection in blood flow. *Phys. Rev. E*, 80(1):016213–1 – 016213–7, July 2009.

[12] UNAIDS. *90–90–90 An ambitious treatment target to help end the AIDS epidemic.* Joint United Nations Programme on HIV/AIDS (UNAIDS), Geneva, Switzerland, 2014.

[13] L. Wang. Global dynamical analysis of HIV models with treatments. *International Journal of Bifurcation and Chaos*, 22(9):1250227–1250238, September 2012.

Abstract

In this thesis a nonlinear analysis is performed in biomedical systems through numerical simulation of two theoretical models of diseases. One of the numerical models used for the study is a modified simplified model of HIV dynamics, with the emergence of opportunistic infections, including two antiretroviral treatments, as well as the study of their effectiveness. The other nonlinear model represents the behavior of blood flow in vessels in the presence of an aneurysm. Through numerical simulation a fluid flow analysis is performed as well as the identification of coherent structures.

The main objective of this thesis is to present an analysis of these simplified nonlinear models by applying nonlinear systems tools. The study also aims to evaluate the mathematical behavior of HIV by infecting immune cells, and the development of opportunistic infections; evaluate the effectiveness of two types of antiretroviral treatments; demonstrate the transition from ordered to chaotic dynamics and their variations in the effectiveness of antiretroviral treatment; numerically simulate blood flow behavior in a simplified blood vessel model with aneurysm, and detect coherent structures from these simulations; to characterize the influence of aneurysm amplitude on the generation of coherent structures, which are responsible for the alteration of blood platelet circulation.

The present work analyzed a modified simplified model for the dynamics of HIV based on Lund *et al.* [25] which describes the nonlinear dynamics of the $CD4^+$ T lymphocyte population and its interaction with HIV. Two types of antiretroviral treatment were included, based on Wang [39].

The results presented for the numerical simulation of blood flow shows that the aneurysm amplitude interferes in the formation of coherent structures. It is possible to observe that a vortex is generated at the beginning of the vessel and over time this vortex is advected and dissipates. Then there is the formation of another vortex, again in the upstream region of the vessel. The other structures evidently formed are well-defined lines, which represent transport barriers. Transport barriers can influence particle agglomeration and clot formation.

Among the conclusions of this work it was found that by reducing the effectiveness of antiretroviral therapy, the nonlinear model exhibits a transition from orderly to chaotic dynamics via a period-doubling cascade. The chaotic regime is interrupted by regions of periodic dynamics known as periodic windows. The results obtained may contribute to the understanding the dynamics of HIV and predict irregular outbreaks of the viral load, as well as the appearance of opportunistic infections.

The numerical study of the theoretical model of the blood vessel with aneurysm

enabled an analysis of the behavior of blood flow within the vessel and how the size of the aneurysm influences the formation of coherent structures.

The formation of coherent structures can cause weakening of the vessel wall, as they can apply pressure and tension at a certain point in the wall by diverting part of the blood flow. This accumulation of flow in a region can influence the rupture of the aneurysm.

This study provides a better understanding of how blood flow works in a vessel with aneurysm, promoting assistance in the diagnosis and treatment of blood pathology.

Keywords: Nonlinear Dynamics; Chaos; Numerical Simulation; Bifurcation; Intermittency; Coherent Structures.

Contents

List of Figures

LIST OF ABBREVIATION

BVS Virtual Health Library, from Portuguese *Biblioteca Virtual em Saúde*

FTLE Finite-Time Lyapunov Exponent

HIV Human Immunodeficiency Virus

ODEs Ordinary Differential Equations

SNB Saddle-Node Bifurcation

List of Symbols

∘   Compound Function

·   Derivative

LIST OF PARAMETERS

P — Population of Non-infected and Non-activated TCD^4 Lymphocytes

X — Non-infected and Activated T_4 Lymphocytes

Y — Infected T_4 Lymphocytes

V — Free HIV Virus

I — Opportunistic Infection

σ_1 — Reverse Transcriptase Inhibitors

$\sigma 2$ — Protease Inhibitors

Λ — The rate of production of P cells

μ — The cell death rate

γ — The rate of cell removal from the pool through cell division of the number of P cells

r — The rate of cell division of X cells

β — The rate of decrease population of activated lymphocytes when the activated cells become infected by HIV

d — The rate of decrease of activated cells by saturation phenomenon

k — The rate of cell division

α — The rate of decrease in the population of Y cells

$\lambda\alpha$ — The rate of new HIV buds from the surface of infected T4 cells

b — The HIV population death rate

δ — The rate of decrease of V through absorption by activated and infected cells

σ — The rate of elimination through the immune response

c — The rate of increase of I trough proliferation

h — The rate of decrease of I through the effect of the immune response

1   Introduction

1.1   Contextualization and Formulation of the Problem

Theoretical models provide reliable means to enable predictions of HIV behavior in defense cells and how the blood flow behaves in the presence of an aneurysm in the blood vessel.

The infection caused by Human Immunodeficiency Virus (HIV) stems from exposure to the retrovirus of the type HIV-1 or HIV-2. The HIV virus damages white blood cells, also known as leukocytes, which are responsible for immunity mediated by antigens. The HIV has as the primary target of auxiliary T lymphocytes, also represented as CD4$^+$ T lymphocytes. The CD4$^+$ T lymphocytes are responsible for coordinating the function of the immune defense system against, mainly, viruses, bacteria and fungus [1] [12] [7].

There is still no treatment available that is able to eliminate HIV from the human body. However, there are treatments that aim to slow down the harmful process caused to the immune system. Examples of antiretroviral therapies include medicines that act as reverse transcriptase inhibitors and protease inhibitors [36].

Reverse transcriptase inhibitors act on the reverse transcriptate enzyme, preventing cell infection from occurring, thus preventing the viral RNA from becoming complementary DNA. Protease inhibitors block the fragmentation of the viral precursor protease enzyme, preventing the maturation of the virus [1].

There are analyses of theoretical nonlinear models that study the relationship between HIV and the immune system, the evolution of infection by HIV associated with the flareup of opportunistic diseases. Some examples of numerical studies can be seen in the publications of Anderson and May [3], Li e Wang [22], Lund *et al.* [25], Perelson *et al.* [30], Wang [39].

There are also numerical studies involving hemodynamic phenomena [33][38]. These studies are of great importance due to the relevant limitations of *in vitro* analyzes and the inability to replicate human blood vessels based on animal models.

Numerical simulation is a technique that makes it possible to perform hemodynamic analysis. Studies using simulation allow the anatomical structure of blood vessels to be

reproduced, in order to observe the influence of pathologies on hemodynamic behavior [4].

Several circulatory diseases can interfere with blood flow performance. One of these pathologies is the aneurysm, which can be characterized as "Pathological outpouching or sac-like dilatation in the wall of any blood vessel (arteries or veins) or the heart. It indicates a thin and weakened area in the wall which may later rupture." [12].

1.2 OBJECTIVES

1.2.1 General Objective

The main objective of this work is to present a theoretical analysis of simplified nonlinear models for biological systems, using tools from nonlinear systems.

1.2.2 Specific Objectives

To achieve the general objective of this work, we carry out a study of nonlinear dynamics that will analyse:

- Theoretical HIV study

  - Numerically simulate a nonlinear model of HIV in the presence of opportunistic infection.
  - Analyze bifurcations and transitions to chaos, according to the effectiveness of the treatment.

- Theoretical study of aneurysm

  - Numerically simulate blood flow in a simplified model of vessel with aneurysm.
  - Detect coherent structures in blood flow.
  - Characterize the influence of aneurysm amplitude on the generation of coherent structures.

1.3 STRUCTURE OF THE DISSERTATION

This chapter refers to the introduction of the work, presentation of the objectives and structure of this dissertation.

Chapter 2 briefly describes nonlinear equations, iterations, fixed points, periodic orbits, Lyapunov exponent, and ends with an explanation of chaotic orbit.

Chapter 3 presents the theoretical study of the Human Immunodeficiency Virus. This chapter has been divided into sections. In the first section the theoretical framework to help understand the virus and its performance within the organism is presented, as well as epidemiological data and numerical studies already carried out on this subject. The following section explains the nonlinear model of HIV in the presence of opportunistic infection, associated with antiretroviral treatment. Then the methodology is described; as well as the numerical results and discussions.

Chapter 4 presents the theoretical study of blood flow in the presence of an aneurysm. This chapter sets out the theoretical framework to help understand the model of an aneurysm in the blood vessel. Then the methodology is described; the numerical results and discussions regarding the numerical simulation of blood flow in the presence of aneurysm.

Finally, chapter 5 addresses the final considerations of this thesis and the perspective for future works.

2 CHAOS

One of the notable mathematical discoveries of the XX century was that simple systems, can behave unpredictably, even if they involve only one variable. This unpredictable behavior was titled "chaos" [14][23].

For chaos to be established there must be unstable behavior. The Lyapunov exponent is used to analyze the irregularity present in the behavior of the points along the iterations. As defined by Alligood [2] "Chaos is defined by a Lyapunov exponent greater than zero". In this chapter, we will address the relationship of chaos with Lyapunov number and Lyapunov exponent .

The essential foundations for Chaos Theory are related to sensitivity to initial conditions and limited predictability. The Chaos Theory is an instrument that assists the analysis of nonlinear dynamic systems. These systems exhibit random and regular behavior [26].

2.1 NONLINEAR EQUATIONS

A quadratic nonlinear equation can be represented by

$$y = mx^2 + n$$

where m and n are parameters.

An example of a nonlinear equation is the quadratic map. This can be defined by:

$$Q_c(x) = x^2 + c$$

where $c \in \mathbb{R}$ is a constant.

Although the quadratic maps seem simple, their dynamics are complicated. The c constant is a parameter in which for each different c it results in a different dynamic system Q_c.

2.2 ITERATIONS

Iteration means, in programming, the repetition of one or more processes systematically. In nonlinear systems the repeated process is the application of a function. Iterating a function suggests evaluating the function several times, using the output from the previous application as input. "Mathematically, this is the procedure of repeatedly composing the function itself" [14].

To exemplify an iteration, we have that, if

$$F(x) = x^2 + 1$$

performing the iterations

$$\text{First iteration: } F(x) = x^2 + 1$$
$$\text{Second iteration: } F^2(x) = (x^2 + 1)^2 + 1$$
$$\text{Third iteration: } F^3(x) = [(x^2 + 1)^2 + 1]^2 + 1$$

then

$$F^2(x) = (F \circ F)(x)$$
$$F^3(x) = (F \circ F \circ F)(x)$$

2.3 FIXED POINTS

Fixed points are values of x such that $F(x) = x$, i.e., the value of x remains constant after performing an iteration of F. In the case of a differential equation, the fixed points reflect an equilibrium solution, it can also be known as a stable, constant or resting solution, as long as it satisfies the condition of $x = x^*$ and $x(t) = x^*$ [14] [35].

The fixed point theorem determines that there is at least one fixed point, under the conditions below. This theorem establishes that if

$$F : [a, b] \rightarrow [a, b]$$

is a continuous function, then there is at least one fixed point of F in $[a, b]$.

Fixed points can be attracting, repelling or neutral. Suppose that x_0 is a fixed point of F, it is considered an attracting when $|F'(x_0)| < 1$. If $|F'(x_0)| > 1$, so x_0 is a repelling fixed point. If $|F'(x_0)| = 1$, the point will be neutral [14].

As definition of a fixed point, we have the following circumstance:

Suppose

$$F(x_0) = x_0$$

then

$$F^2(x_0) = F[F(x_0)]$$
$$F^2(x_0) = F[x_0]$$
$$F^2(x_0) = x_0$$
$$F^n(x_0) = x_0$$

For this example, the orbit can be identified as $\{x_0; x_0; x_0; ...; x_0\}$.

Fixed points can also be found geometrically by analyzing the intersection of the graph with the diagonal line $y = x$, where $F(x) = y$ [14].

A point is occasionally fixed or occasionally periodic if it is neither fixed nor periodic, but at some point in the orbit it is fixed or periodic [14].

Figure 2.1 shows fixed points by means of graphs. The representation of attracting fixed points is shown in Figure 2.1a. The arrows indicate that the points approach the origin from the iterations. In Figure 2.1b, the arrows move away, indicating repelling points.

2.4 PERIODIC ORBITS

By definition, the term orbit can be defined according to Devaney [14] as:

"Given $x_0 \in \mathbb{R}$, we define the orbit of x_0 under F to be the sequence of points $x_0; x_1 = F(x_0); x_2 = F^2(x_0); ...; x_n = F^n(x_0)$. The point x_0 is called the seed of the orbit."

Therefore, the point x_0 will be periodic if $F^n(x_0) = x_0$ for $n > 0$, where n is the main period of the orbit. If x_0 is periodic with the period n, the orbit of x_0 will be a repeated sequence of values.

Figure 2.2 is a graphical representation of a periodic orbit, where any point leads to the same situation.

The periodic orbit is related to the periodic fixed point, where the periodic fixed point of period n is attracting if it is an attracting point of F^n, and will be repelling if it is a repelling fixed point of F^n.

6
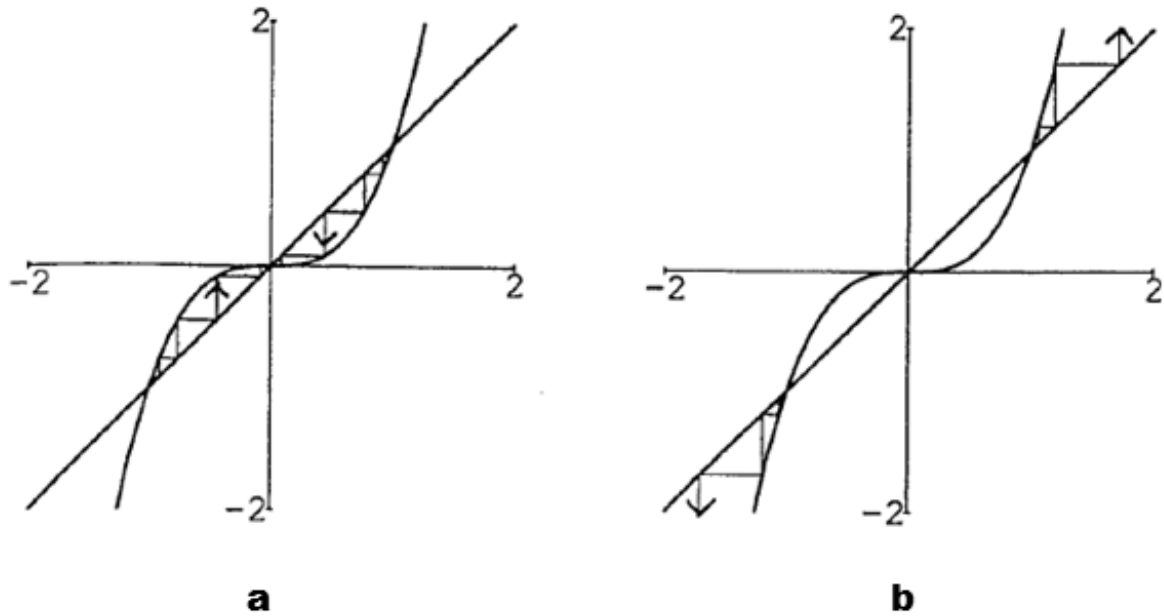
Figure 2.1. Graphical representation of fixed points, for $a.|x| < 1$ and $b.|x| > 1$.
Fonte:[14]
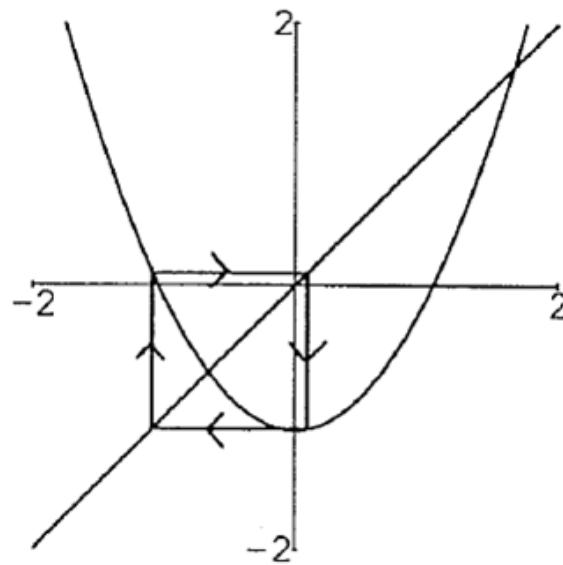
Figure 2.2. Graphical representation of a periodic orbit.
Fonte:[14]

2.5 SADDLE-NODE BIFURCATION

The solutions of nonlinear equations can change stability depending on the control parameters. For example, the quadratic map presents a type of bifurcation in $c = \frac{1}{4}$. This bifurcation is known as the Saddle-Node Bifurcation (SNB).

The bifurcation can be defined as follows: "Whether $F(\lambda)$ is a family of functions with a parameter λ, we say that $F(\lambda)$ undergoes a tangential bifurcation, or saddle-node,

at $\lambda = \lambda_0$, if there is an open interval I and a $\epsilon > 0$, such that:

1. For $\lambda e \,] \lambda_0 - \epsilon, \lambda_0 \,[$, $F\lambda$ has no fixed points.

2. For $\lambda = \lambda_0$, $F\lambda$ has a neutral fixed point.

3. For $\lambda \,\epsilon\,] \lambda_0, \lambda_0 + \epsilon \,[$, $F\lambda$ has two fixed points, an attracting and a repelling.

It is possible to invert the sequence of the intervals in topics 1, 2 and 3. Making $F\lambda = F\lambda^n$ we have that periodic points can also undergo tangential bifurcations" [14].

2.6 LYAPUNOV EXPONENT

The Lyapunov number and Lyapunov exponent can be stipulated according to the description of Alligood [2]: "Let f be a continuous function in $\mathbb{R}$, the number of Lyapunov $L(x_1)$ from the orbit $\{x_1, x_2, x_3 \,...\,\}$ is defined as:

$$L(x_1) = \lim_{n \to \infty} (|f'(x_1)| \,... \,|f'(x_n)|)^{1/n}$$

if this limit exists.

Lyapunov exponent can be defined as:

$$\lambda(x_1) = \lim_{n \to \infty} (1/n)[\ln |f'(x_1)| + ... + \ln |f'(x_n)|]$$

if this limit exists. Note that λ exists if and only if L exists and is non-zero, and $\ln L = \lambda$."

Therefore, the Lyapunov number is by definition the average change of rate of the distance from the nearby points along the entire length of the orbit. The Lyapunov exponent is the natural logarithm of the number of Lyapunov [2].

Lyapunov exponent measures the rate of convergence or divergence from the initial conditions. A positive λ_i indicates that two nearby solutions will diverge exponentially with time, whereas a negative value indicates exponential convergence. Each exponent represents the exponential divergence/convergence rate of solutions along a different direction in the phase space. In the case of continuous-time dissipative dynamical systems modelled by a set of Ordinary Differential Equations (ODEs) at least one exponent is always equal to zero. For this reason we will focus on the maximum non-zero Lyapunov exponent, represented by λ_{MAX}. The dynamics are chaotic if $\lambda_{\mathrm{MAX}} > 0$. If $\lambda_{\mathrm{MAX}} < 0$ and there is only one vanishing Lyapunov exponent, then the dynamics are periodic. If $\lambda_{\mathrm{MAX}} < 0$ and there is two or more vanishing Lyapunov exponents, then the dynamics are quasiperiodic.

8

Figure 2.3 is a graphical representation in which the first iterations have similar values, and then, over the course of some iterations, the difference between their values increases.

Figure 2.3. Lyapunov Exponent
Fonte:[14]

2.7   CHAOTIC ORBIT

The term chaos originates from the Greek ($\chi\acute{\alpha}o\varsigma$ khaos) which has a meaning of abyss or emptiness [11]. Chaos Theory, or Complex Systems Theory, is used in numerous studies, such as engineering, geophysical, biological and epidemiological [8] [22] [25] [30]. Chaos is part of the content of the dynamics. It is one of several alternative behaviors of a nonlinear system. There are several definitions in the literature for the behavior of a disordered dynamic system, ranging from exponential separation of orbits to positive Lyapunov exponent [21] [32] [35].

For this work, the definition of Alligood [2] is considered, in which chaos can be defined as:

"Let f be a function of $\mathbb{R}$, and let $x_1, x_2, ...$ be a f bounded orbit. The orbit is chaotic if:

1. $\{ x_1, x_2, ... \}$ is not asymptotically periodic.

2. The Lyapunov exponent is greater than zero."

Therefore, the chaotic orbit, which is not exactly fixed or periodic, exhibits an unstable behavior, susceptible to initial conditions.

According to Devaney [14], if the function $F : \mathbb{R} \to \mathbb{R}$ is continuous and if F has a periodic point of period 3, then F will have periodic points of all types of period. Consequently, it is established that period 3 leads to chaos.

Figure 2.4 is a graphical representation of a chaotic orbit.
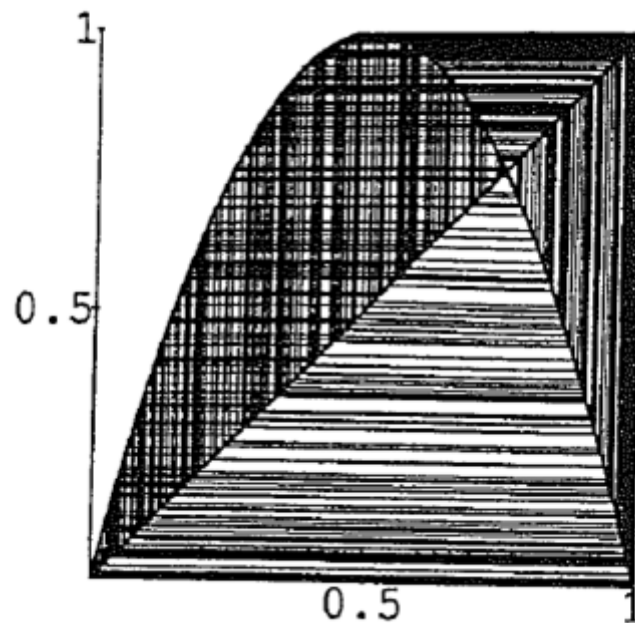
Figure 2.4. Chaotic Orbit
Fonte:[14]

2.8 Poincaré surface of section

The Poincaré surface of section is a tool commonly used in dynamical system analysis to simplify the analysis of continuous-time models such as Equations (3.1)-(3.5). The numerical solutions of ODEs form a continuous set usually called a trajectory, orbit or flux. The five-dimensional space spanned by the variables (P, X, Y, V, I) is called the phase space.

A Poincaré surface of section is a "plane" defined in phase space which intersects the trajectory of the system. By focusing on the intersecting points the analysis of a five-dimensional continuous set of solutions can be simplified to a four-dimensional discrete set of points. The discrete set of points lying on the Poincaré plane are called Poincaré points.

For example, Figure 2.5(a) shows the phase space projected onto the (V, I) plane. The continuous line represents a particular numerical solution of Eqs. (3.1)-(3.5). A Poincaré plane defined by

$$I = 120V,$$

is represented by a dashed line. The intersections between the trajectory and the Poincaré plane such that $\dot{V} < 0$ (i.e., in the direction which V decreases) are indicated by red circles. Figure 2.5 shows the time series of V and the sequence of Poincaré points corresponding to Figure 2.5(a). From this figure it is evident that the behavior of the continuous-time solution (in this case, a period-4 trajectory) can be clearly elucidated from the sequence of Poincaré points. Periodic solutions will be represented by a periodic sequence of points, whereas chaotic solutions are identified by a sequence of points that never repeats.

Figure 2.5. (a) The phase space projected on the (V, I) plane. The continuous line represents a trajectory, the dashed line is the Poincaré section, and red circles show the selected intersections between the trajectory and the section. (b) The corresponding time series (black) and the Poincaré points as a function of time.
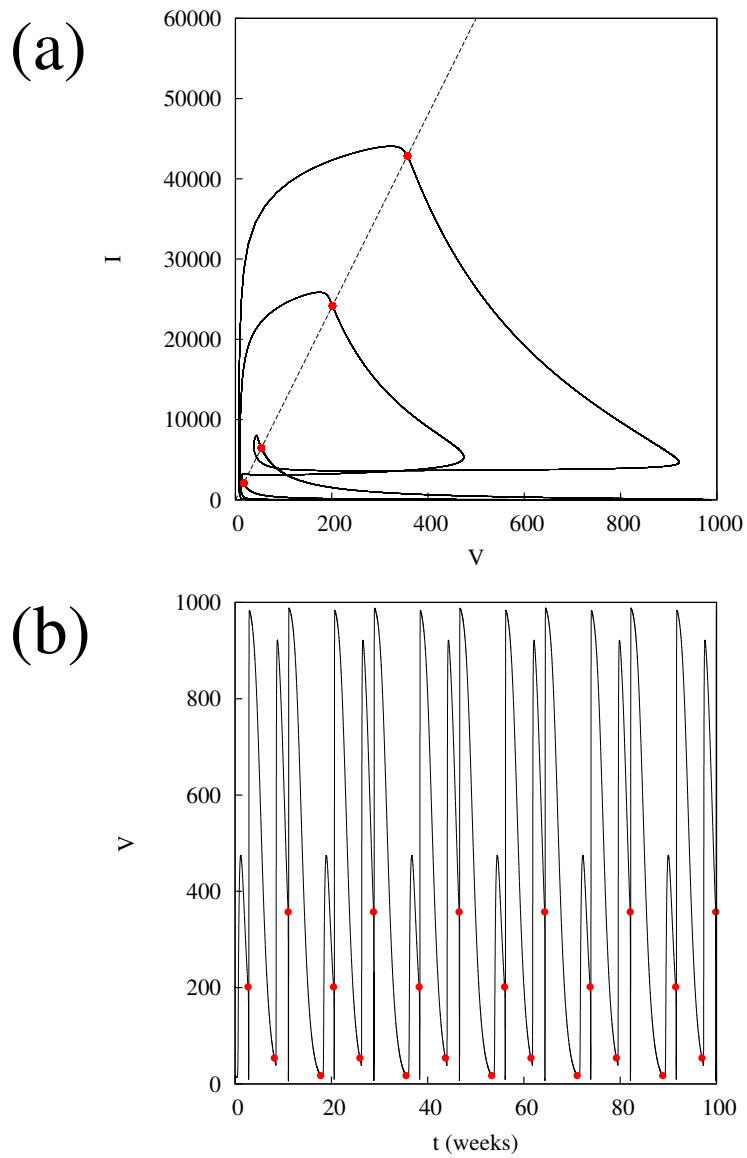
3   Human Immunodeficiency Virus

3.1   Theoretical Framework

HIV is a historical non-taxonomic term that refers to either of the two species, HIV-1 and HIV-2 [12].

The HIV has as main target the $CD4^+$ T lymphocytes. The HIV virus connects to the receptor in cell, fusion of virus with the cell occurs. After the release of the viral material, retroviral RNA is used as a template for the manufacture of DNA, because of the action of the enzyme reverse transcriptase. The DNA is formed on a single strand and after its formation, the RNA is degraded. The DNA is free in the cytoplasm, and with the aid of reverse transcriptase it makes DNA single stranded in double helix DNA. The DNA formed will be integrated into the host cell's DNA with the help of the integrase enzyme. Viral protein is produced and new viral RNAs are formed. The protease enzyme is responsible for breaking the precursor viral protein into smaller, and mature proteins. The RNA and proteins are released to infect other cells [1] [9].

The medicines that inhibit these enzymes prevent the multiplication of HIV in the body. These medicines are called antiretrovirals.

This virus promotes the cellular depletion of $CD4^+$ T lymphocytes. These cells mature in the thymus and are responsible for coordinating the immune response against microorganisms, for example, viruses. The reduction of $CD4^+$ T cells results in widespread damage to the functioning of the immune system as a whole. The weakened organism becomes more susceptible to the appearance of opportunistic infections. Among the most common infections are herpes simplex, cryptosporidiosis, pneumonia, cryptococcosis and toxoplasmosis [1].

Global statistics released by the Joint United Nations Program on HIV/AIDS [37] estimated that in the year 2017 some 36.9 million people are living with HIV worldwide. Based on these statistics, it is necessary to further study the progression of the disease, as well as the most effective treatment and opportunistic diseases that may arise.

Theoretical studies can contribute to our understanding of the dynamics of the HIV virus. Several studies have focused on nonlinear models that describe the interaction

between HIV and immune cell populations, in particular CD4$^+$ T lymphocytes.

For example, Anderson and May [3] proposed a simplified model that explains the complex dynamic behavior between HIV and the immune system. This model was studied by Lund *et al.* [25] that demonstrated that the dynamics of the virus can become chaotic through a cascade of periodic duplication. Perelson *et al.* [30] analyzed a model of three populations of designated as T cells, uninfected T cells, infected and latent T cells and active and infected T cells, and their interaction with the free virus. They demonstrated that the cytopathicity of HIV is an important factor that leads to the quantitative characteristics of HIV infection. Wang [39] studied the mathematical model HIV with uninfected T cells, infected T cells and free virus.

Their study associated the interaction between the HIV virus and CD4 $^+$ T cells with treatments, reverse transcriptase inhibitors and protease inhibitors. Li and Wang [22] studied a mathematical model that describes the viral dynamics of HIV with antiretroviral treatments.

These studies demonstrated that numerical studies of nonlinear models can provide reliable predictions about the interaction between HIV and the immune system and the development of HIV and opportunistic diseases, in addition to helping to determine the most appropriate treatment and contribute to the public policy development.

This work can contribute to the most appropriate intervention to be stipulated by public policies aimed at the treatment and viral suppression of people infected with HIV, predicting the number of infected cells, viral load and antiretroviral efficacy [5] [36].

3.2 Nonlinear Model of HIV

The study consists of a modified simplified model of the dynamics of HIV in the presence of an opportunistic infection. The effect of two antiretroviral treatments is also included.

3.3 Methodology

The present work analyzed a modified simplified model based on Lund *et al.* [25] which describes the nonlinear dynamics of the CD4$^+$ T lymphocyte population uninfected and not activated cited as P, from uninfected and activated CD4$^+$ T lymphocyte as X, CD4$^+$ T lymphocytes infected as Y, free HIV virus as V and opportunistic infection like I. According to Wang [39], antiretroviral treatment was included by inserting two parameters, represented as σ_1 and σ_2, which represent the reverse transcriptase inhibitors and the protease inhibitor, respectively. The physical interpretation of σ_1 and σ_2 is given

below. The model is described by the following set of Ordinary Differential Equations

$$\dot{P} = \Lambda - \mu P - \gamma PV, \qquad (3.1)$$

$$\dot{X} = \gamma PV + rX - \beta XV - dX^2 + kIX, \qquad (3.2)$$

$$\dot{Y} = \sigma_1 \beta XV - \alpha Y, \qquad (3.3)$$

$$\dot{V} = \sigma_2 \lambda \alpha Y - bV - \delta(X + Y)V - \sigma XV, \qquad (3.4)$$

$$\dot{I} = cI - hIX, \qquad (3.5)$$

where Λ represents the rate of production of P cells, μ represents the cell death rate, γ is the rate of cell removal from the pool through cell division of the number of P cells, r is the rate of cell division of X cells, β represents the rate of decrease population of activated lymphocytes when the activated cells become infected by HIV, d is the rate of decrease of activated cells by saturation phenomenon, k is the rate of cell division, α stands for the rate of decrease in the population of Y cells, $\lambda \alpha$ is the rate of new HIV buds from the surface of infected T4 cells, b represents the HIV population death rate, δ is the rate of decrease of V through absorption by activated and infected cells, σ is the rate of elimination through the immune response, c represents the rate of increase of I trough proliferation, h represents the rate of decrease of I through the effect of the immune response, σ_1 involves inhibitors reverse transcriptase and σ_2 involves protease inhibitors.

Equations (3.1)-(3.5) are obtained by describing the interaction between T cells and HIV virus using a nonlinear predator-prey model. These models can successfully reproduce several characteristics observed in infected patients such as long transient periods of dormancy, depletion of healthy T cells and exponential grow rates of HIV virus and opportunistic infections [3][25][30]. Following Lund *et al.* [25] we set the model parameters as $\Lambda = 1.0$, $\mu = 0.1$, $\gamma = 0.01$, $r = 1.0$, $\beta = 1.0$, $d = 0.001$, $k = 0.01$, $\alpha = 2.0$, $\lambda \alpha = 10.0$, $b = 1.0$, $\delta = 0.01$, $\sigma = 0.1$, $c = 1.0$, $h = 0.01$.

The effectiveness of reverse transcriptase inhibitor treatment is given by $1 - \sigma_1$ and the effectiveness of protease inhibitor treatment is given by $1 - \sigma_2$ [39]. A value of $\sigma_1 = 0$ represents 100% effectiveness of reverse transcriptase inhibitor treatment, whereas $\sigma_1 = 1$ represents 0% effectiveness. Similarly, a value of $\sigma_2 = 0$ represents 100% effectiveness of protease inhibitor treatment, whereas $\sigma_2 = 1$ represents 0% effectiveness. Note that the σ_1 parameter can be also interpreted as the probability that an activated T cell become infected. Lund *et al.* [25] showed that equations (3.1)-(3.5) exhibit a period-doubling route to chaos when σ_1 increases. In this thesis we focus on the effect of the antiretroviral treatment, therefore we set $\sigma_1 = 1$ and let σ_2 be the control parameter.

The numerical integration of equations (3.1)-(3.5) is performed using the `lsoda` package which is a variable-step integrator [31]. The initial conditions are $P = X = Y = V = I = 0.1$.

3.4 NUMERICAL RESULTS AND DISCUSSION

Figure 3.1 shows the time series of the P, X, Y, V and I variables as a function of time, for $\beta = 0.1$, $\sigma_1 = 1$ and $\sigma_2 = 1$, i.e., in the absence of treatment. Figure 3.1 the red color represents the opportunistic infection, the blue the activated lymphocytes, the pink the infected lymphocytes, and the green the free virus. In this regime the dynamics is periodic, characterized by large-amplitude fluctuations triggered by the presence of the opportunistic infection I [25].

When an opportunistic infection arises, lymphocytes are activated, increasing the population of these cells to fight the infection. This increase in these populations is also related to the increase in infected lymphocytes, and consequently the increase in free virus. Note that when the population of the opportunistic infection (I) increases, the number of activated lymphocytes X grows and is followed by the infected lymphocytes (Y) and the population of HIV virus (V). Equations behave as expected with what happens in reality.

The Figure 3.2 corresponds to the maximum Lyapunov exponent in terms of σ_1 and σ_2. The color scale indicates chaotic dynamics, in contrast, the gray scale characterizes periodic oscillations. Within the chaotic region there are periodic bands, also known as "periodic streets" [27]. One of these "streets" is highlighted by arrows, and will be the focus of the subsequent analysis.

Then, the effectiveness of the treatment with reverse transcriptase inhibitors (σ_1) on the dynamics of HIV was investigated.

The upper left panel of the Figure 3.3 depicts the bifurcation diagram of the virus population V to $\sigma_1 \in [0, 1]$ and $\sigma_2 = 1$. This panel 3.3 shows a route similar to the chaos described by Lund *et al.* [25] in terms of the β parameter. We now focus on σ_1 alone.

The bifurcation diagram was constructed by defining the Poincaré surface of the section $I(t) - 40V(t) = 0$ and $\dot{I} > 0$ in the variable space and selecting the points of the equations orbit. (3.1) - (3.5) that intersect with the Poincaré section.

Asymptotic solutions were obtained by discarding the initial transitional points up to $t = 1000$. The chaotic regime ($\sigma_1 > 0.4$) is occasionally interrupted by periodic windows.

This bifurcation diagram demonstrates that the dynamics of the virus can become unpredictable if the effectiveness of treatment with a reverse transcriptase inhibitor (σ_1)
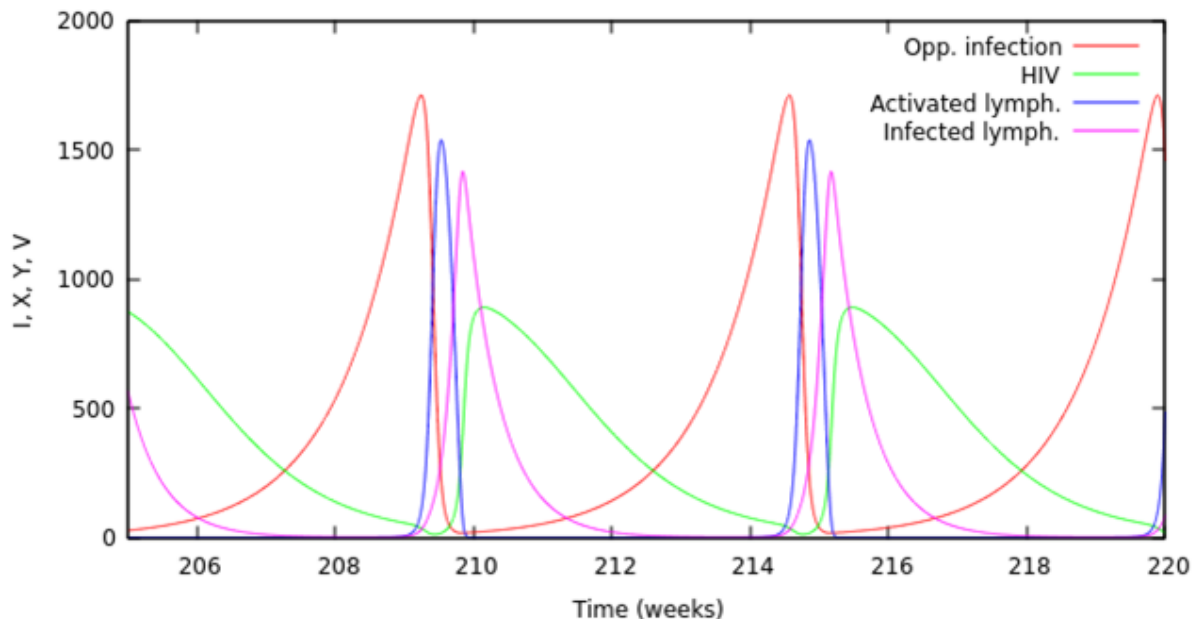
Figure 3.1. Time series of the population of the opportunistic infection (red), the population of free HIV (green), the population of activated lymphocytes (blue) and the infected lymphocytes (cyan) for $\beta = 0.1$ and $\sigma_2 = 1$. On the y axis I is an arbitrary unit, X and Y are represented by cells/mm^3, and V are virions.

is reduced.

In order to validate the different regimes displayed by the bifurcation diagram, maximum Lyapunov exponent other than zero [40] was calculated as a function of the σ_1 bifurcation parameter. The result is shown in the lower left panel of the Figure 3.3. It is evident that the periodic dynamics is characterized by $\lambda_{\mathrm{MAX}} < 0$, while the chaotic behavior corresponds to $\lambda_{\mathrm{MAX}} > 0$ as expected.

The upper right panel of Figure 3.3 is an enlargement of a period window 12. The lower right panel represents the subsequent enlargement of the upper branch, indicated by the arrow in the upper right panel of the figure.

The upper panel of the Figure 3.4 represents the time series of the dynamics of the free virus, V, where the Poincaré points are represented. Exposing a regular behavior interrupted by intermittent chaotic bursts to $\sigma_1 = 0.483510$. The lower panel, on the other hand, depicts the time series with a more elongated regular behavior and with chaotic bursts shortened to $\sigma_1 = 0.483634$.

When the value of σ_1 is greater, distancing from the saddle-knot point, the regular intervals are greater. This allows for greater predictability in relation to the increase of the free virus in the body.

The Figure 3.5 shows the relation of the average time (τ) between the intermittent events (black circles) as a function of the distance of σ_1 from the SNB in the chaotic
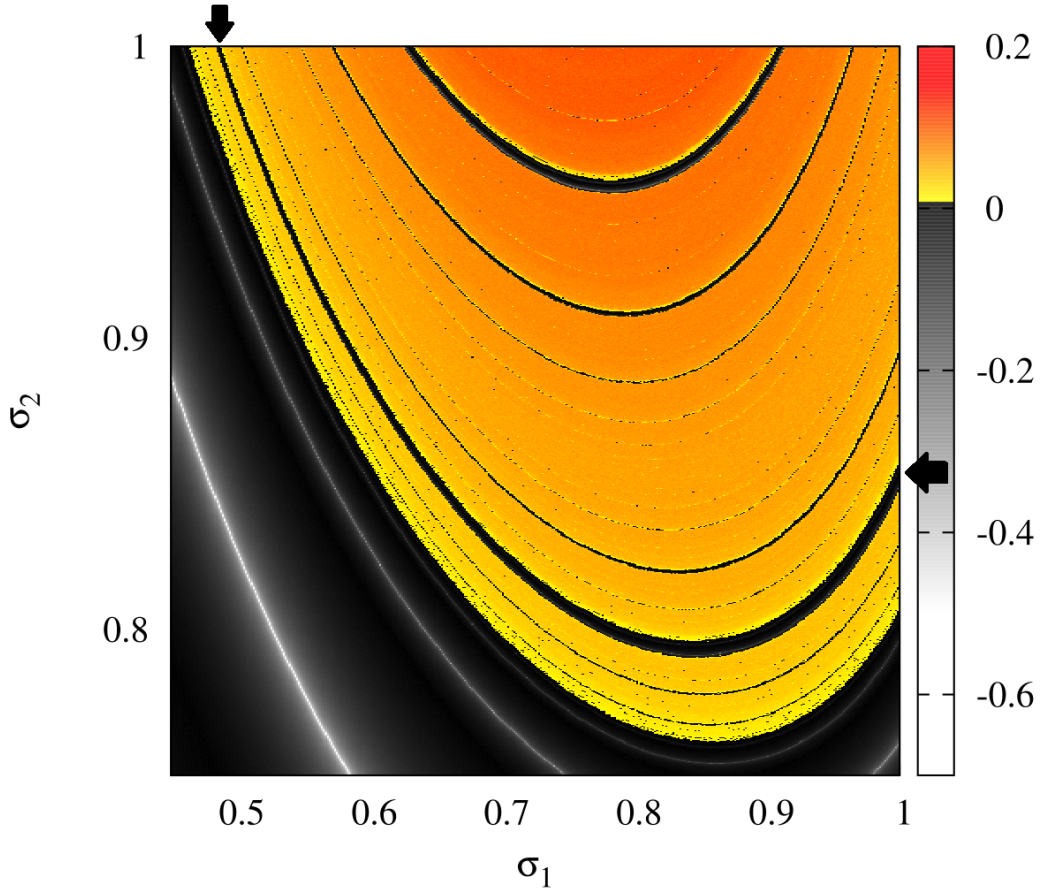
17

Figure 3.2. Maximum Lyapunov exponent as a function of σ_1 and σ_2. The color scale indicates chaotic dynamics, while the gray scale indicates periodic oscillations. Arrows indicate "periodic streets".

regime. The *tau* is the distance between the bifurcations. The dashed line determines the power law with the slope $\gamma = \text{-}0.35 \pm 0.02$ on the log-log scale. In view of this, when the distance between σ_1 and the saddle-node bifurcation decreases, the average time of regular intervals increases; thus following the power law.

From the investigation of the efficacy of treatment with protease inhibitor (σ_2) the results described below were obtained.

Figure 3.6 shows in the upper left panel the bifurcation diagram of the virus population V for $\sigma_2 = [0, 1]$ and $\sigma_1 = 1$. The bifurcation diagram was elaborated by determining the Poincaré surface of the section $I(t) - 40V(t) = 0$ and $\dot{I} > 0$ in the variable space and selecting the points of the equations orbit (3.1) - (3.5) that intersect with the Poincaré section. Asymptotic solutions were obtained by discarding the initial transitional points up to $t = 1000$.

This bifurcation diagram 3.6, as well as the one in Figure 3.3 shows a route similar to chaos, also characterized by Lund *et al.* [25].
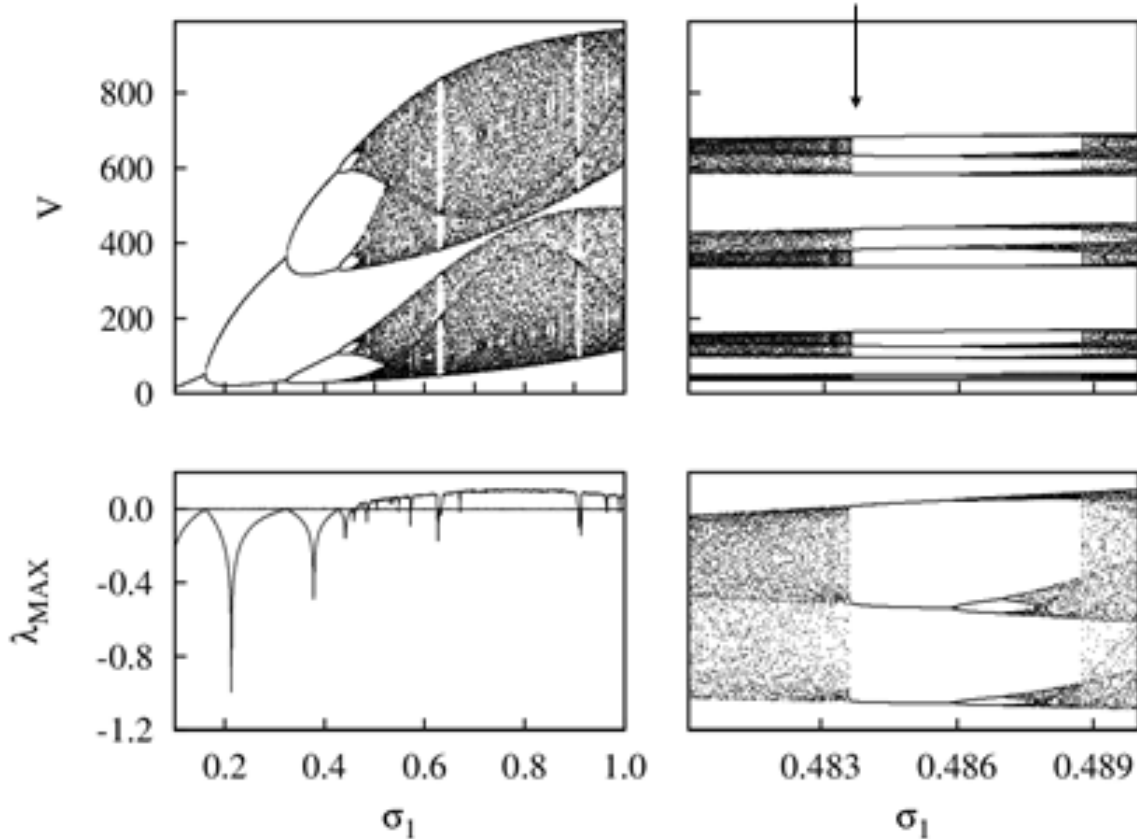
Figure 3.3. Top left panel: Bifurcation diagram for V based on σ_1. Lower left panel: Maximum Lyapunov exponent based on σ_1. The horizontal line indicates the value zero. Upper right panel: Detailed view of a period 12 window. Lower right panel: an increase in the upper branch.

At $\sigma_2 \sim 0.05$, the orbit converges to a limit cycle represented by a period 1 attractor. At $\sigma_2 \sim 0.2$, the limit cycle period is doubled. By increasing the value of σ_2 (that is, decreasing the effectiveness of treatment with protease inhibitors), the dynamics of the virus undergoes a cascade that doubles the period. At $\sigma_2 \sim 0.8$, the dynamics of the virus become chaotic.

In the same way as in Figure 3.3, the bifurcation diagram for σ_2 shows that with the decrease in the efficiency of the treatment, the dynamics of the virus can become unpredictable.

In order to validate the different regimes shown by the bifurcation diagram, the maximum non-zero Lyapunov exponent [40] [24] was calculated as a function of the bifurcation parameter σ_2. The result is shown in the lower panel of the Figure 3.6. Periodic dynamics are characterized by $\lambda_{\text{MAX}} < 0$, while the chaotic behavior corresponds to $\lambda_{\text{MAX}} > 0$ in line with expectations.

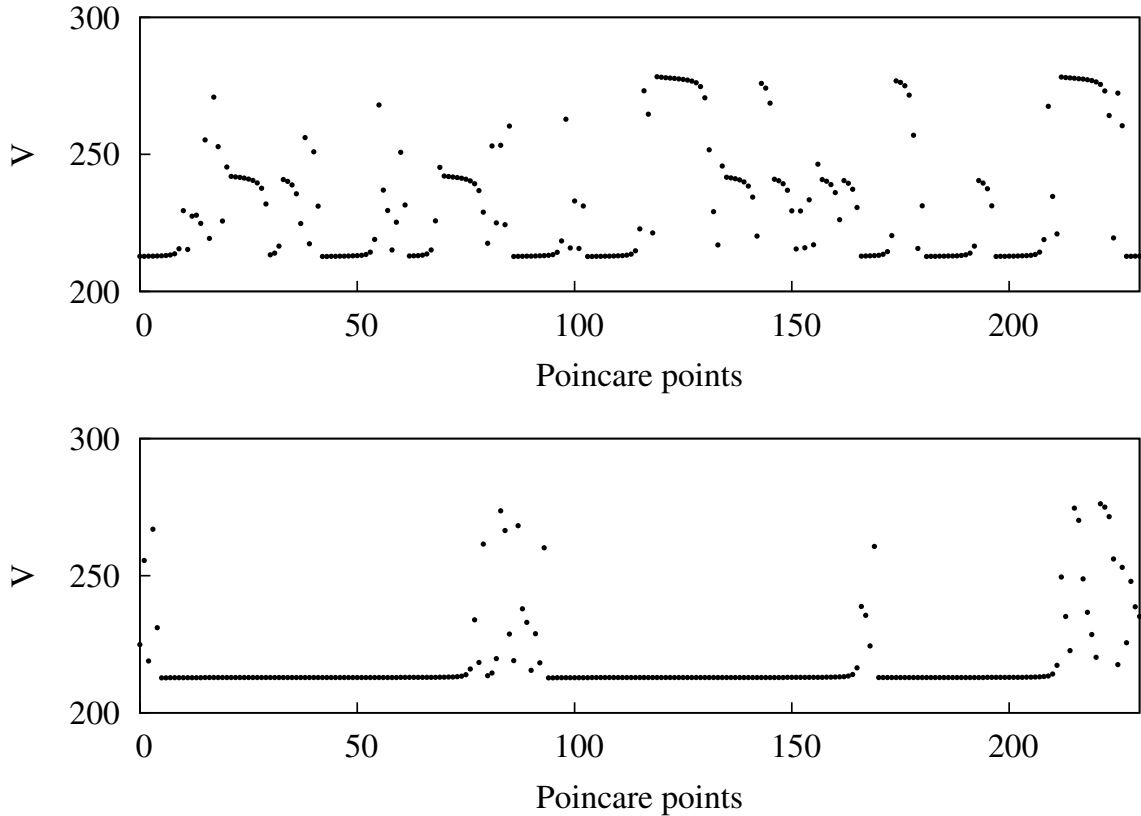In the same way as performed in Figure 3.3, an increase of a periodic window of

Figure 3.4. Top panel: Time series of V showing regular behavior interrupted by intermittent chaotic bursts, for $\sigma_1 = 0.483510$. Lower panel: at $\sigma_1 = 0.483634$, the time series exhibits a longer regular behavior and chaotic bursts are shorter.

period 12 was performed to detail that window. This magnification can be seen in the upper right panel of the Figure 3.6. The upper branch of the upper right panel was enlarged, marked with an arrow in the Figure 3.6.

We note that in Figure 3.3 the virus dynamics becomes chaotic at $\sigma_1 \sim 0.47$, whereas in Figure 3.6 the corresponding chaotic state appears at $\sigma_2 \sim 0.8$. This means that the virus dynamics become unpredictable if the effectiveness of the RT inhibitor is reduced to 53 % in the absence of the P inhibitor, or if the effectiveness of the P inhibitor is reduced to 20 % in the absence of the RT inhibitor.

Figure 3.7 shows the relation of the average time (τ) between the intermittent events (black circles) as a function of the distance of σ_2 from the saddle-node bifurcation in the chaotic regime. The dashed line determines the power law with the slope $\gamma = -0.39$ $\pm$ 0.04 on the log-log scale. Thus, when the distance between σ_2 and the saddle-node bifurcation decreases, the average time of regular intervals increases, thus following the power law.

Figure 3.5. Average time τ between intermittent events (black circles) as a function of the distance of σ_1 from the saddle-node bifurcation in the chaotic regime. The dashed line indicates that the power law fits with the slope $\gamma = -0.35 \pm 0.02$ on the log-log scale.
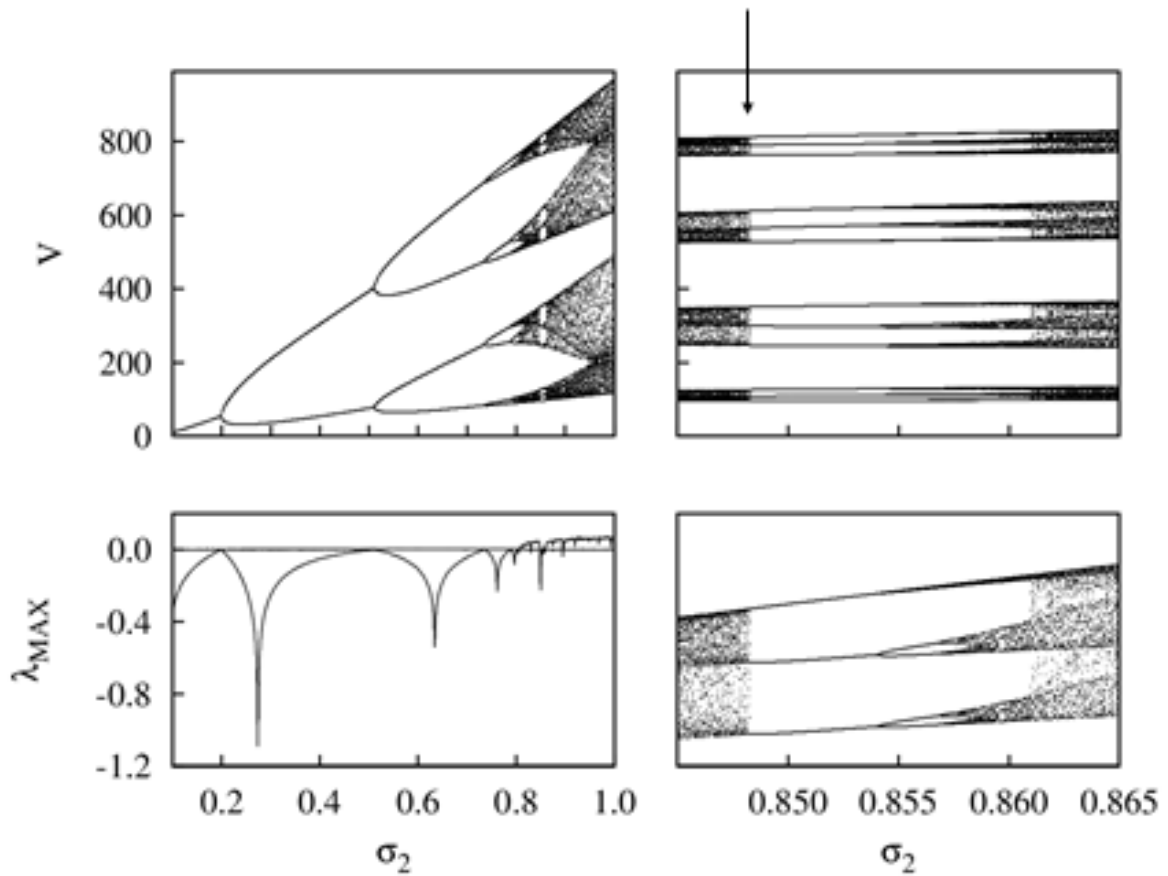
Figure 3.6. Top left panel: Bifurcation diagram for V based on σ_2. Lower left panel: Maximum Lyapunov exponent as a function of σ_2. The horizontal line indicates the value zero. Upper right panel: Detailed view of a period 12 window. Lower right panel: an increase in the upper branch.
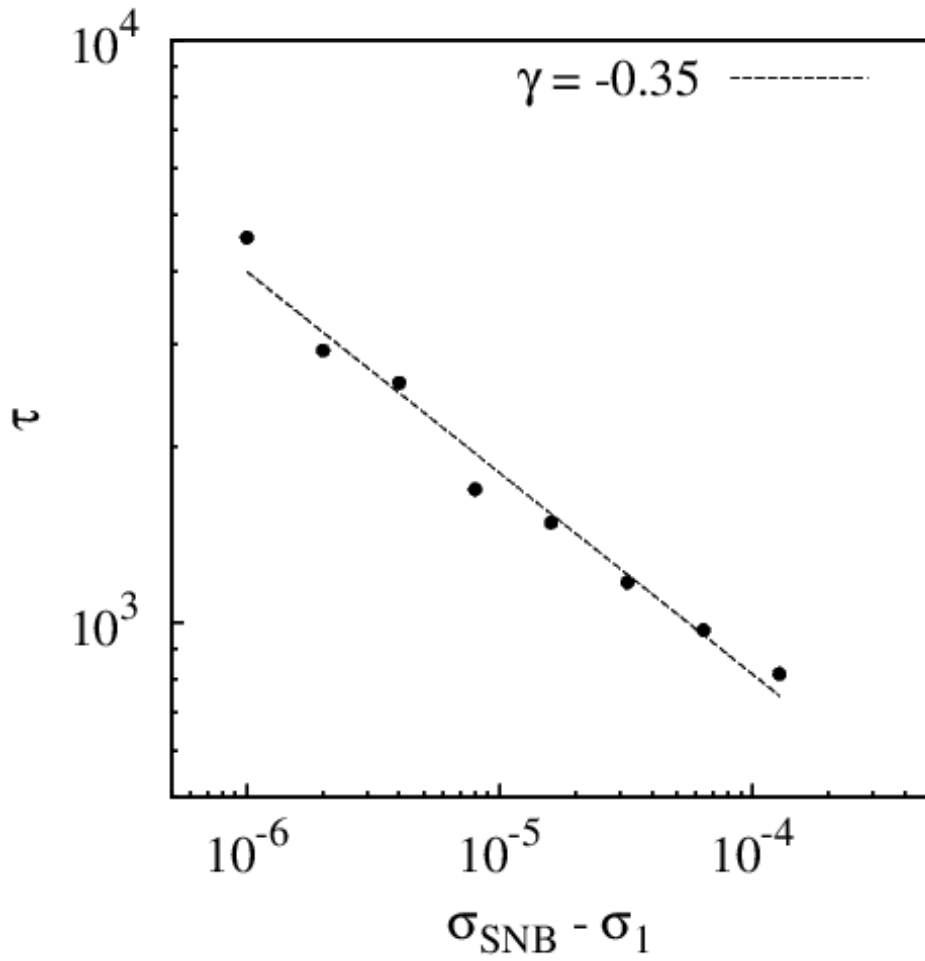
Figure 3.7. Average time τ between intermittent events (black circles) as a function of the distance of σ_2 from the saddle-node bifurcation in the chaotic regime. The dashed line indicates that the power law fits with the slope $\gamma = $ -0.39$\pm$ 0.04 on the log-log scale.
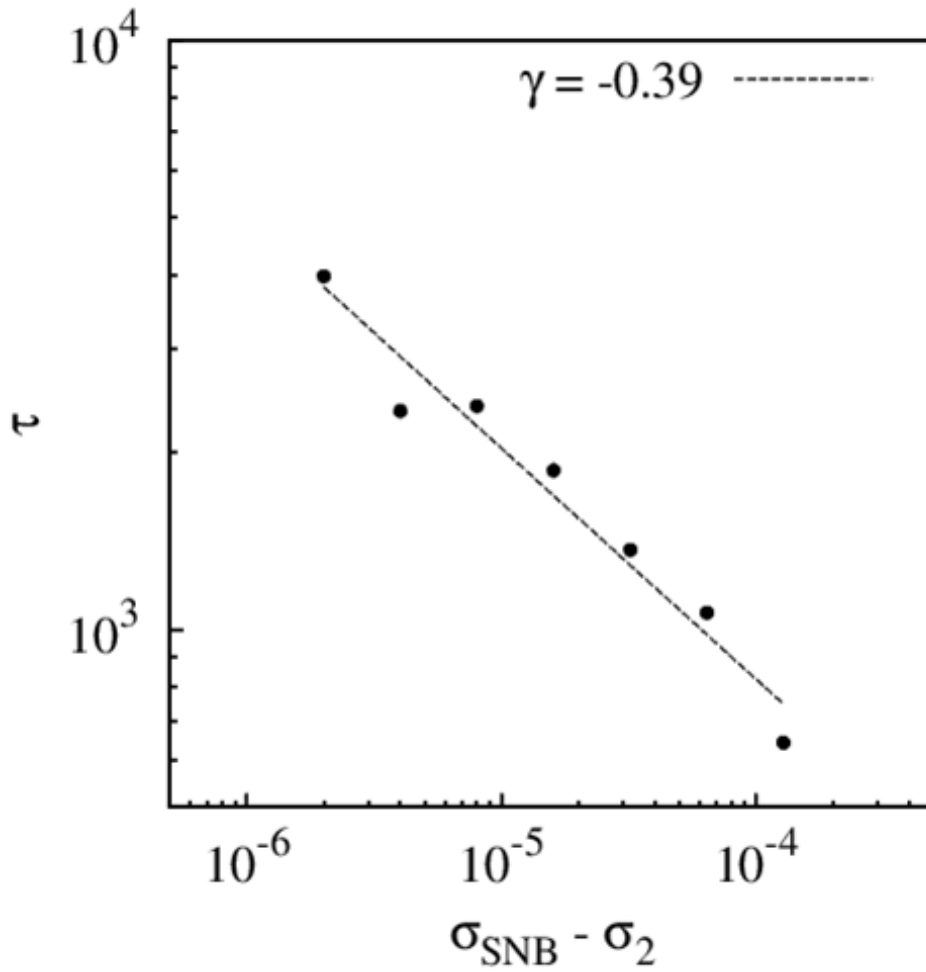
4   NUMERICAL SIMULATION OF BLOOD FLOW

4.1   THEORETICAL FRAMEWORK

The study of hemodynamic phenomena associated with computer simulation techniques is extremely important for understanding the functioning of blood movement and the development of circulatory diseases that can influence the behavior of blood flow, such as aneurysms.

According to Virtual Health Library, from Portuguese *Biblioteca Virtual em Saúde* (BVS), the concept of aneurysm can be defined as: "Pathological evacuation or saculiform dilation in the wall of any blood vessel or in the heart that may rupture later." [12].

Aneurysms can be caused by atherosclerosis, hypertension, trauma, infection or congenital weakness in the vessel wall. Frequently the aneurysms come into view in the aorta, but may appear in the peripheral vessels. The aneurysm formed, there is pressure and cutting tensions that the blood flow exerts on the vessel wall. This promotes a gradual expansion of the aneurysm due to the fragility of the vessel wall with an aneurysm. When the dilated vessel wall does not resist the stresses resulting from the internal blood flow, the aneurysm ruptures[6] [13].

Computer simulation is a technique that allows hemodynamic studies in a viable, inexpensive and fast way because numerical codes are used to predict blood flow behavior under any circumstances. Through it it is possible to carry out virtual interventions with the purpose of assisting diagnosis and treatment. Studies using this simulation technique make it possible to reproduce the anatomical structure of blood vessels, in order to analyze the influence of pathologies on hemodynamic behavior [4].

Due to the significant limitations of *in vitro* studies and the inability to replicate the variable anatomy of human blood vessels from animal models, this work aims to analyze blood flow in the presence of circulatory diseases through computer simulation. In order to provide better understanding, diagnosis and treatment of blood disorders.

The Reynolds number is defined as

$$R = \frac{L \cdot V}{v}, \tag{4.1}$$

where L and V being respectively a characteristic scale and velocity of the flow, and v its kinematic viscosity[15].

The Reynolds number is used to differentiate whether the regimes are turbulent or laminar. The high value of Reynolds number represents a turbulent regime, while a low value represents a laminar regime[15].

The flow can present different behaviors depending on the characteristics of the fluid and the dimensions of the channel, with different classifications such as laminar, periodic, or turbulent. In addition, particles submerged in the fluid can follow chaotic trajectories, even in the presence of a laminar fluid [10] [15].

Turbulent blood flows can generate filamentary structures that catalyze the activity of reagent particles, which can lead to the acceleration of biochemical processes, making certain particles easier to agglomerate, such as platelets [33].

The detection of filamentary structures in turbulent fluids is a topic of great interest in the scientific community. Several techniques have been proposed to separate random fluctuations from persistent coherent structures. A promising proposal has recently been developed using Lagrangian techniques, that is, using a frame that moves along with a particle, and that one moves along with the fluid.

A coherent structure would be defined as a material line, that is, a "hurdle" in the fluid that prevents the passage of a tracer from one region of the fluid to another. This barrier is called the Lagrangian coherent structure [18] [34] and has been shown to be useful to understand the chaotic mixing processes in turbulent fluids, where the velocity field has spatial and temporal dependence [19] [28].

The Lagrangian coherent structure in two-dimensional turbulence is interested with patterns emerging from the advection of passive tracers. The dynamical behavior of tracers is more affected by phase space geometry in Lagrangian methods for turbulence. [20] [29].

According to Haller and Yuan [20], a Lagrangian coherent structure is defined as " ...regions of qualitatively different tracer dynamics. Such regions can be best approached by following the mixing of passive tracers. An initially regular passive tracer blob tends to reveal nearby coherent structures through stretching, thinning, and folding around them...Lagrangian coherent structure boundaries are defined as material lines with locally the longest or shortest stability or instability time."

4.2 Model of Aneurysm

The study consists of a numerical model of a simplified blood vessel in the presence of an aneurysm. The identification of coherent structures according to changes in fluid behavior due to variations in the size of the aneurysm are objects of this study.

4.3 Methodology

This work numerically simulated the aneurysm in a blood vessel. To perform the simulation, a simplified model of a blood vessel in the presence of an aneurysm was elaborated using the Comsol Multiphysics software. This software solves the equations that describe the dynamics of the fluid. These equations are detailed in Appendix A.

The representation of this model is depicted in the Figure 4.1. In this model, G indicates the amplitude of the aneurysm. The arrow on the left represents the entry of blood flow into the vessel, and the arrow on the right represents the exit of blood flow. The dashed line indicates that there is a mirroring image of the vessel, because it was considered a axisymmetric aneurysm model, that is, all the processes performed in the upper region of the vessel were also performed in the lower region.
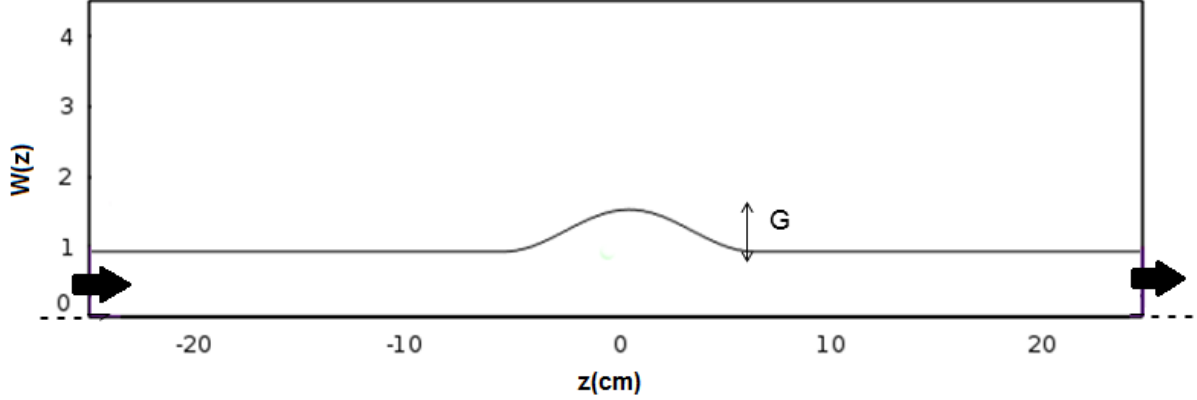

Figure 4.1. Representation of the simplified model of the blood vessel in the presence of an aneurysm, where the arrows indicate the entry and exit of the flow; G represents the amplitude of the aneurysm; and the dashed line indicate the mirroring image of the vase.

The model can be mathematically described as follows. The walls of the vessel are given by a piece wise function

$$W(z) = \begin{cases} 1, & -25 \leq z < -L \\ 1 + G \cdot (1 + \cos(z \cdot \frac{\pi}{L})), & -L \leq z < L \\ 1, & L \leq z < 25 \end{cases}$$

26

where $L = 6cm$. All length units are in cm.

The heart pumps blood through cyclical movements. These movements are contraction, known as systole, and relaxation, known as diastole. The cardiac cycle is composed of cardiac events that happen from the beginning of one beat to the beginning of the next beat [16][17]. For this analysis, the cardiac cycle was considered to last approximately 1 second. The cardiac cycle is represented in the model through the input blood flow. The blood flow enters the vessel from the left boundary with a velocity given by

$$V_{in}(t) = 7 \cdot (4t)^2 \cdot \frac{e^{-(4t)^2}}{10} \cdot \sin\left(\frac{\pi \cdot 4t}{2}\right) + 0.1, \qquad (4.2)$$

where t represents time in seconds. The flow exists the vessel through the right boundary. The flow properties are set to mimic a blood flow (*i.e.*, a non-Newtonian flow at body temperature and atmospheric pressure). The details are given in Appendix A.

Equation 4.2 is represented by the Figure 4.2. The heartbeat is represented in Figure 4.2. Approximately every 1 second the cardiac cycle is repeated, therefore showing that it is periodic.
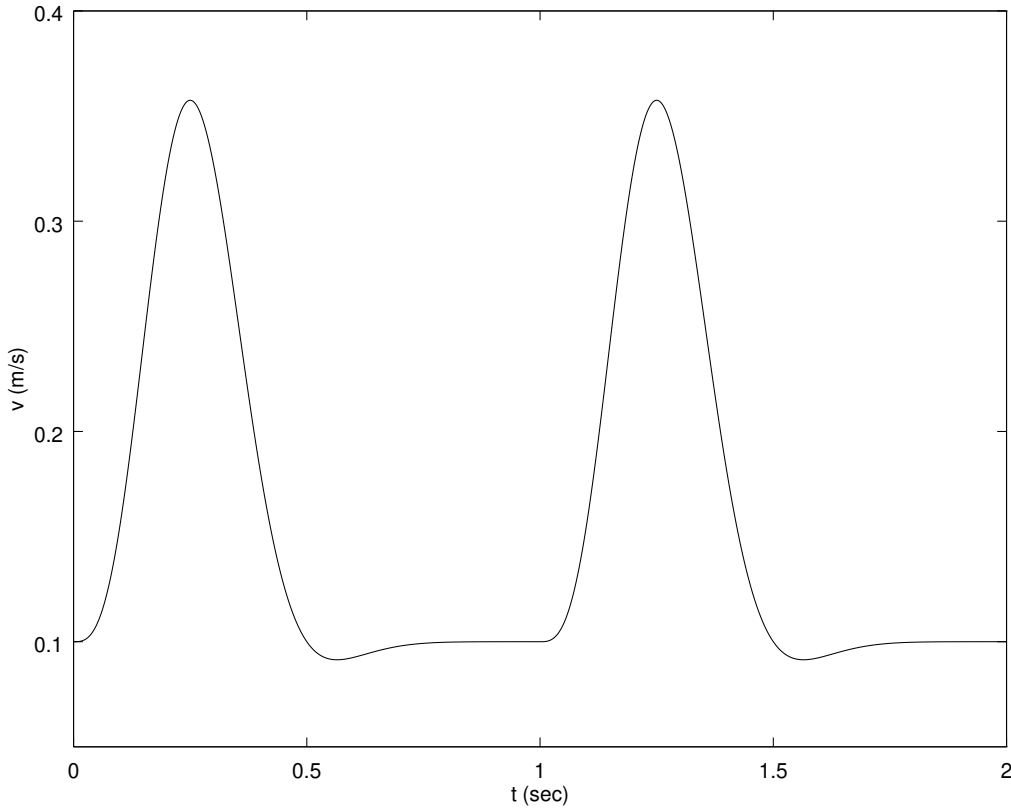

Figure 4.2. Representation of the input blood flow velocity in the vessel

27

In the Figure 4.3, the "finer mesh" was selected and an amplification was made in the aneurysm region. Each point in mesh represents a variable. This amplification was carried out with the purpose of facilitating the identification and representation of coherent structures, both vortexes and filaments.
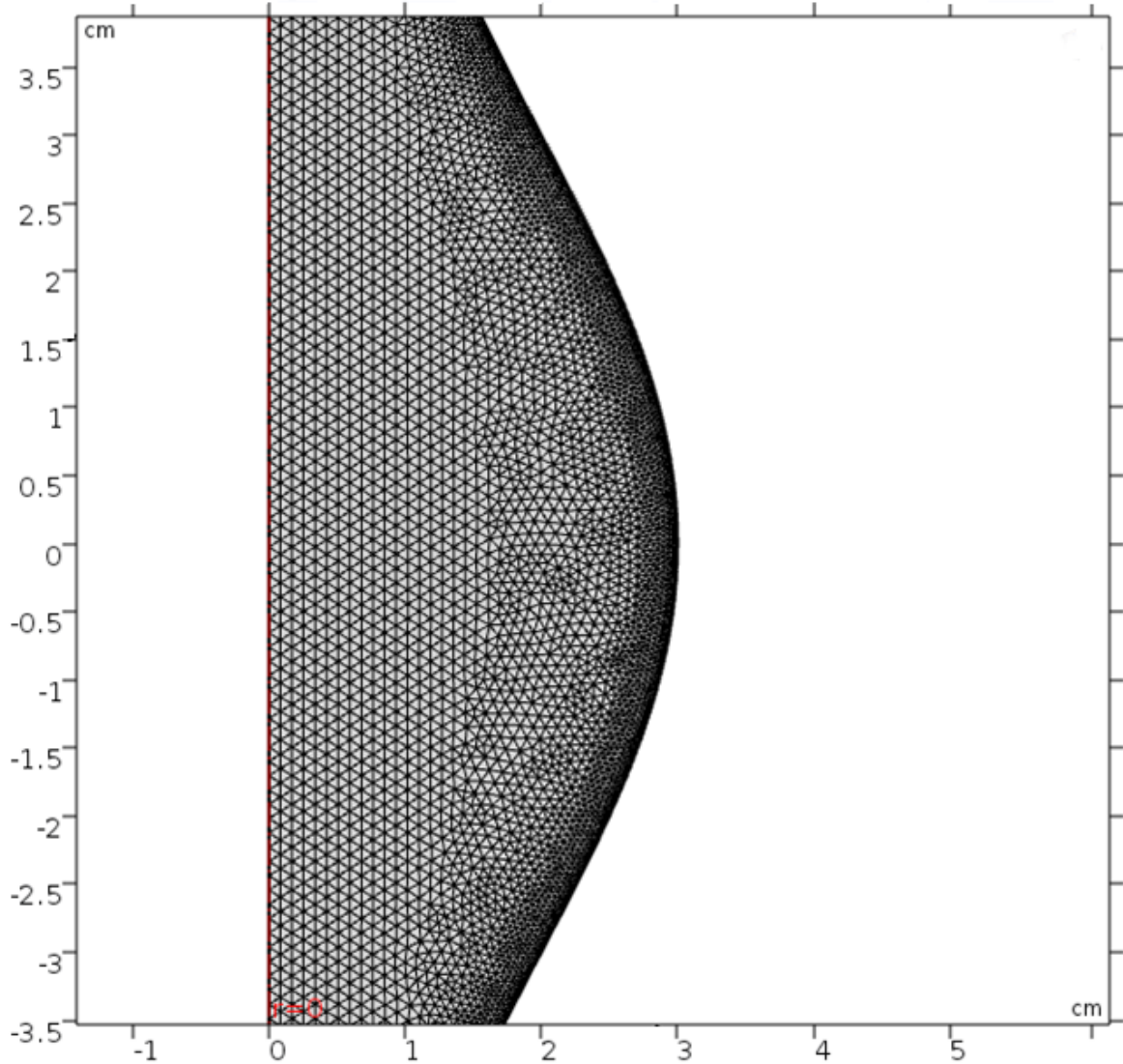
Figure 4.3. Aneurysm amplification in "finer mesh"

The analysis of the blood flow velocity was performed for each amplitude of the selected aneurysm with the use of Comsol Multiphysics software. Variations in blood flow behavior and the formation of coherent structures will be observed. For analysis, the times corresponding to the beginning of the cardiac cycle, diastole and systole, were selected. Where $t = 0$ seconds corresponds the beginning of the cardiac cycle, $t = 0.625$ seconds represents the diastole, and $t = 1.25$ seconds describes the systole.

4.4 Numerical Results and Discussion

Through the analysis on a simplified numerical model of blood vessels in the presence of an aneurysm, based on Schelin *et al.* [33] and Varghese [38], the following results were obtained.

Figure 4.4 shows the portrait of the blood velocity $|V|$ in a vessel with the presence of an aneurysm, for $G = 0.2, 0.6, 1.0$ and 1.4 cm, and $t = 0$ seconds, corresponding the beginning of the cardiac cycle. This figure shows the behavior of $|V|$ as the aneurysm increases. Each panel represents a different amplitude of the aneurysm, where the upper left panel has an amplitude of 0.2 cm; the top right panel has 0.6 cm; the lower left panel has 1.0 cm; and the lower right panel has 1.4 cm.
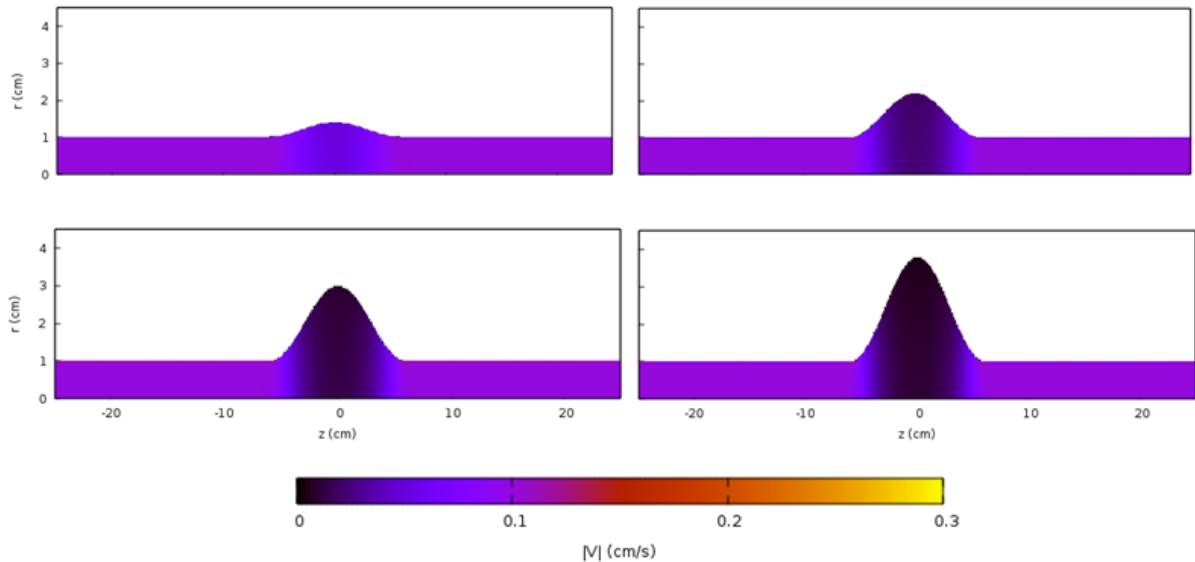
Figure 4.4. Flow velocity representation in the blood vessel with aneurysm for different amplitudes (G) for time $= 0$s. Upper left panel: $G = 0.2$. Upper right panel: $G = 0.6$.Lower left panel: $G = 1.0$. Lower right panel: $G = 1.4$.

Figure 4.5 is similar to Figure 4.4 for $t = 5$ seconds, representing the systole. The behavior of $|V|$ is also demonstrated as the aneurysm increases in amplitude. Each panel represents a different amplitude of the aneurysm, where the upper left panel has an amplitude of 0.2 cm; the top right panel has 0.6 cm; the lower left panel has 1.0 cm; and the lower right panel has 1.4 cm.

Figure 4.6 shows the FTLE for G $= 0.2$ cm, $\tau = 1.0$ and $t_0 = 0.0$, 0.4, 0.8 and 1.2 seconds. The value of τ depends on the systems under study. A small value of τ will not allow the formation of patterns in the FTLE field, whereas a large value of τ implies a higher computational effort. For the simulations of blood flow, several values of τ were tested. We found that values of $\tau > 1.0$ allow for the identification of structures in the FTLE field. From this sequence it is clear that a vortex is formed upstream of
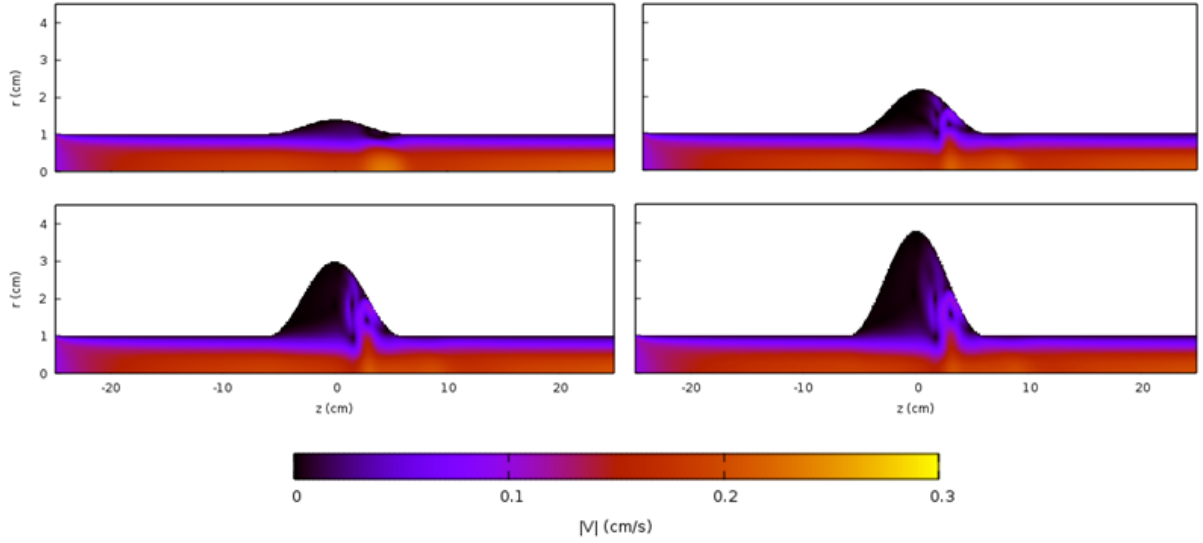
29

Figure 4.5. Flow velocity representation in the blood vessel with aneurysm for different amplitudes (G) for time $= 1.25$ s. Upper left panel: $G = 0.2$ cm. Upper right panel: $G = 0.6$ cm. Lower left panel: $G = 1.0$ cm. Lower right panel: $G = 1.4$ cm.

the aneurysm. This vortex is advected downstream and is dissipated. Note that a new vortex is being formed at the end of the sequence, which indicates that the formation of vortices is a cyclic process, following the cardiac cycle.
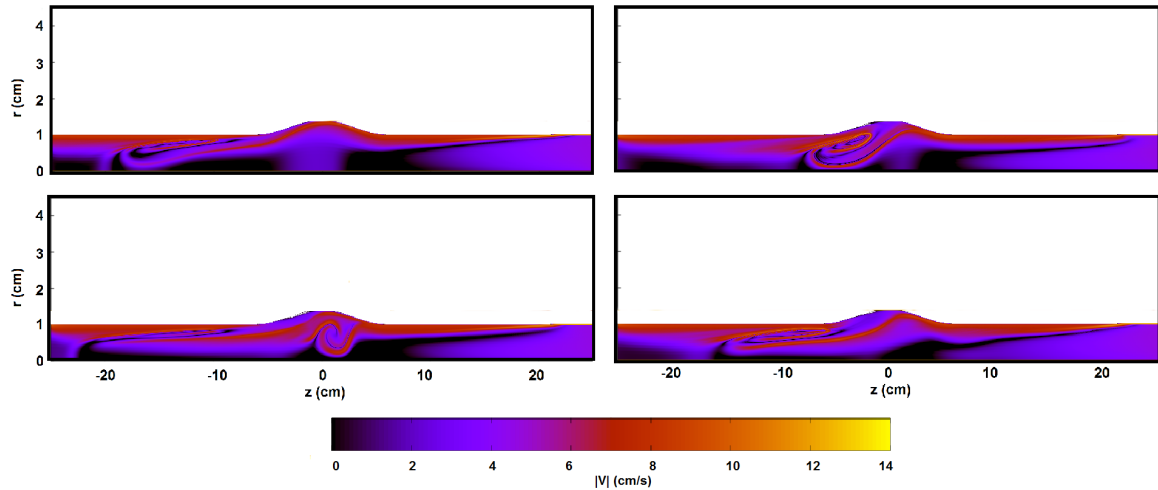
Figure 4.6. FTLE representation in the blood vessel with aneurysm for $G = 0.2$ cm. Upper left panel: $t_0 = 0.0$ s. Upper right panel: $t_0 = 0.4$ s. Lower left panel: $t_0 = 0.8$ s. Lower right panel: $t_0 = 1.2$ s.

Figure 4.7 shows the Finite-Time Lyapunov Exponent (FTLE) for G = 0.2, 0.6, 1.0, and 1.4 cm, $\tau = 1.5$, and $t_0 = 0.625$ seconds, representing the diastole. The FTLE is represented by a color scale. Lower values are indicated by dark colours, whereas light colours represent higher values. Regions of higher FTLE values represent transport barriers which typically appear as contours or "ridges" of the FTLE field. For G = 0.2

cm, the ridges of the FTLE field encircle a point near the central region of the vessel, indicating the presence of a vortex. For G = 0.6 cm, the ridges form filaments encircling a vortex structure that can be clearly distinguished. For G = 1.0 cm, the vortex coexists with entangled ridges surrounding it, reflecting apparently the turbulence of the fluid. For G = 1.4 cm, more entangled ridges appear, and a faint second vortex appears inside the aneurysm. From these figures it is clear that a vortex is form for all values of G. The location of the center of the vortex changes slightly to the right with increasing G, and remains near the center of the vessel.

Figure 4.7. FTLE representation in the blood vessel with aneurysm for different amplitudes (G) for time = 0.625 s. Upper left panel: $G = 0.2$ cm. Upper right panel: $G = 0.6$ cm. Lower left panel: $G = 1.0$ cm. Lower right panel: $G = 1.4$ cm.

Figure 4.8 is similar to Figure 4.7, for t = 1.25 seconds. For G = 0.2 cm, a vortex is being formed upstream of the aneurysm. For G = 0.6, 1.0 and 1.4 cm similar filamentary structures appear. These filaments become more entangled as G increases, and the patterns become increasingly complex. Note that for G = 1.0 and 1.4 small-scale vortices are formed at either side of the filament near the wall inside the aneurysm.
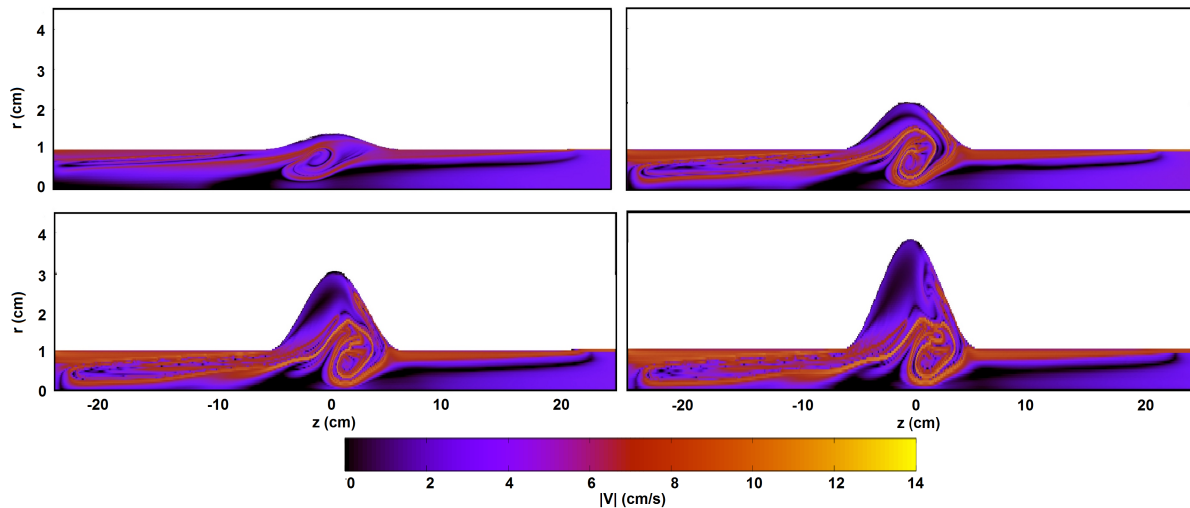
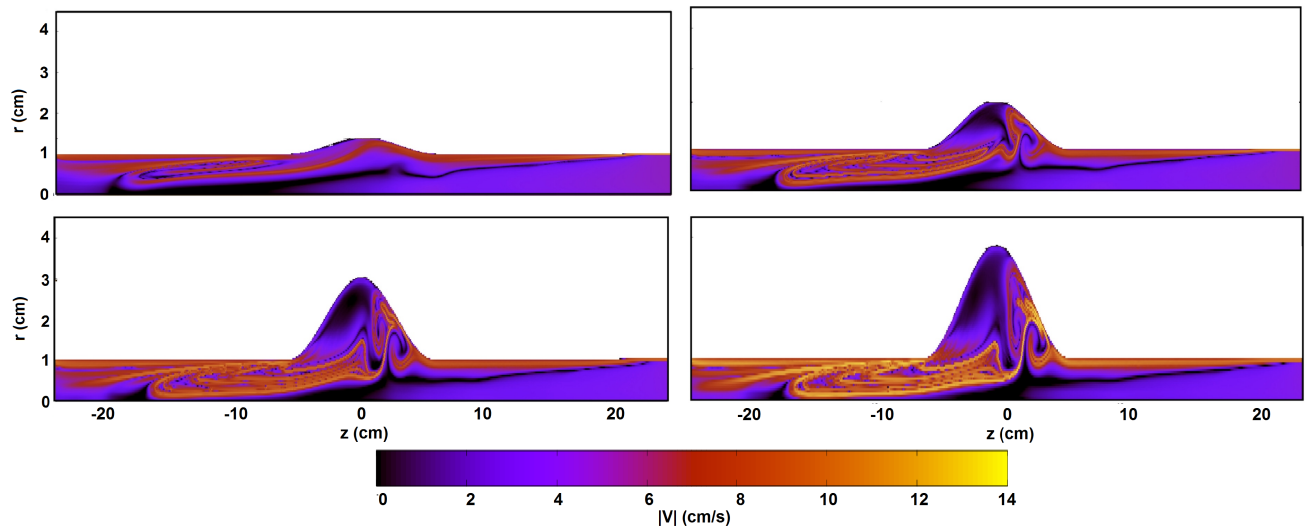**Figure 4.8.** FTLE representation in the blood vessel with aneurysm for different amplitudes (G) for time $= 1.25$s. Upper left panel: $G = 0.2$ cm. Upper right panel: $G = 0.6$ cm. Lower left panel: $G = 1.0$ cm. Lower right panel: $G = 1.4$ cm.

5   CONCLUSION

Through the numerical study of the nonlinear model of HIV dynamics, including antiretroviral treatment and an opportunistic infection, it was possible to analyze the effectiveness of treatment from pre-established parameters.

By decreasing treatment efficiency, a transition from regular to chaotic dynamics was observed through a periodic doubling cascade, leading to a chaotic regime. The chaotic regime is occasionally interrupted by periodic windows. The calculation of the maximum non-zero Lyapunov exponent demonstrates the transition from dynamic (periodic) to irregular (chaotic).

These results can contribute to understanding the dynamics of HIV and predicting irregular bursts of HIV, such as the progression of infection. In addition, it can assist in the definition of public policy protocols focused on HIV treatment.

The numerical study of the theoretical model of the blood vessel with aneurysm enabled an analysis of the behavior of blood flow within the vessel and how the size of the aneurysm influences the formation of coherent structures. It is possible to observe the vortex formation in the model. The fluid generates a vortex at the beginning of the vessel and over time this vortex dissipates. Then there is the formation of another vortex, again in the initial region of the vessel.

The other structures evidently formed are well-defined lines, creating transport barriers. Transport barriers can influence particle agglomeration and clot formation. There is also the formation of entangled within the aneurysm, with the increased amplitude.

The location of the formation of coherent structures can influence in weakening of the vessel wall, as they cause pressure and tension at a certain point in the wall by diverting part of the blood flow. This accumulation of flow in a region can influence the rupture of the aneurysm, the most severe form of the pathology, which can cause death.

This study provides a better understanding of how blood flow works in a vessel with aneurysm, promoting assistance in the diagnosis and treatment of blood pathology. Analysis of this model requires more detailed studies, by changing the parameters of the model equations.

5.1 Recommendation for Future Research

- It is suggested to continue the theoretical study on chaos with other types of antiretroviral treatments;

- Nonlinear modeling for HIV immunization;

- Numerical simulation of blood flow in the presence of stenosis;

- To change the parameters of the model equations;

- Identification the excitation signal of the cardiac cycle system within a vessel with aneurysm.

Publised Contents

de Sousa Moreira L., Cerda R.A.M., de Amorim R.G.G. (2020) **Route to Chaos in a Nonlinear Model of HIV Dynamics with Antiretroviral Treatment**. In: González Díaz C. et al. (eds) VIII Latin American Conference on Biomedical Engineering and XLII National Conference on Biomedical Engineering. CLAIB 2019. IFMBE Proceedings, vol 75. Springer, Cham. https://doi.org/10.1007/978-3-030-30648-9$_9$2

de Sousa Moreira L. **Route to Chaos in a Nonlinear Model of HIV Dynamics with Antiretroviral Treatment**. Oral presentation in VIII Latin American Conference on Biomedical Engineering and XLII National Conference on Biomedical Engineering, Cancún, México.

References

[1] A. K. Abbas, A. H. Lichtman, and S. Pillai. *Imunologia Celular e Molecular*. Elsevier Editora Ltda., Rio de Janeiro, RJ, 9ª edition, 2019.

[2] K. T. Alligood, T. D. Sauer, and J. A. Yorke. *Chaos: An Introdution to Dynamical Systems*. Springer-Verlag New York, Inc, New York, 1996.

[3] R. M. Anderson and R. M. May. *Complex dynamical behavior in the interaction between HIV and the immune system. In Cell to Cell Signalling: From Experiments to Theoretical Models*. Academic Press, Belgium, 1989.

[4] B. M. C. Azevedo. *Estudo preliminar da hemodinâmica em modelos simplificados de aneurismas saculares*. Dissertação de mestrado, Mestrado Integrado em Engenharia Mecânica, Faculdade de Engenharia da Universidade do Porto, 2010.

[5] L. E. Bain, C. Nkoke, and J. J. N. Noubiap. UNAIDS 90-90-90 targets to end the AIDS epidemic by 2020 are not realistic: comment on "Can the UNAIDS 90-90-90 target be achieved? A systematic analysis of national HIV treatment cascades". *BMJ Glob Health*, 2(2):807–817, March 2017.

[6] C. S. S.Cardoso. *Estudo do Comportamento Biomecânico de Aneurismas Cerebrais*. Dissertação de mestrado, Escola Superior de Tecnologia e Gestão, Instituto Politécnico de Bragança, 2015.

[7] E. R. Cachay. *Infecção pelo vírus da imunodeficiência humana (HIV). Manual MSD: versão para profissionais de saúde. Merck Sharp & Dohme Corp, New Jersey, 2018.*

[8] A. R. M. Carvalho. *Epidemiological Models for the Transmission of HIV/AIDS and Relevant Coinfections*. Tese de doutorado, Doctoral Program in Applied Mathematics. Mathematics Department, University of Porto, 2018.

[9] Z. Cheng and A. Hoffmann. A stochastic spatio-temporal (sst) model to study cell-to-cell variability in hiv-1 infection. *Journal of Theoretical Biology*, 395(21):87–96, April 2016.

[10] P. A. Davidson. *Turbulence: an introduction for scientists and engineers.* Oxford Univ. Press., New York, 1ª edição, 2004.

[11] R. de A. Nogueira, P. F. L. Souza, and R. F. de A. A. Oliveira. Transdiciplinaridade e a Física Moderna e Contemporânea: Relatos de Experiências Didáticas. *Revista Inter-Legere*, 1(16):214–242, April 2016.

[12] Health Sciences Descriptors: DeCS. BIREME / PAHO / WHO, São Paulo, SP, rev. and enl. ed. edition, 2017.

[13] W. E. DeTurk and L. P. Cahalin. *Fisioterapia Cardiorrespiratória: Baseada em Evidências.* Ed. Artmed, 1ª edition, 2007.

[14] R. A. Devaney. *A First Course In Chaotic Dynamical Systems: Theory And Experiment.* Avalon Publishing, New York, 1ª edition, 1992.

[15] U. Frisch. *Turbulence, the legacy of A. N. Kolmogorov.* Cambridge University Press., Cambridge, 2004.

[16] L. S. García and D. M.Arteaga. *Soporte Vital Avanzado (Reanimación Cardiopulmonar Avanzada).* Editorial MAD, Sevilla, 1ª edition, 2006.

[17] A. C. Guyton and J. E. Hall. *Fisiologia Medica.* Elsevier Health Sciences, Italy, 12ª edition, 2012.

[18] G. Haller. A variational theory of hyperbolic Lagrangian coherent structures. *Physica D: Nonlinear Phenomena*, 240(7):574–598, March 2011.

[19] G. Haller and F. J. Berón-Vera. Geodesic theory of transport barriers in two-dimensional flows. *Physica D: Nonlinear Phenomena*, 241(20):1680–1702, October 2012.

[20] G. Haller and G. Yuan. Lagrangian coherent structures and mixing in two-dimensional turbulence. *Physica D: Nonlinear Phenomena*, 147(3-4):352–370, December 2000.

[21] M. W. Hirsch, S. Smale, and R. L. Devaney. *Differential Equations, Dynamical Systems and An Introduction to Chaos*, volume 60. Elsevier Academic Press, California, 2004.

[22] M. Y. Li and L. Wang. Backward bifurcation in a mathematical model for HIV infection in vivo with anti-retroviral treatment. *Nonlinear Analysis Real World Applications*, 17(1):147–160, 2014.

[23] L. S. . Liebovitch. *Fractals and chaos simplified for the life sciences.* Oxford University Press, New York, 1998.

[24] E. N. Lorenz. Compound windows of the Hénon-map. *Physica D: Nonlinear Phenomena*, 237(13):1689–1704, August 2008.

[25] O. Lund, E. Mosekilde, and J. Hansen. Periodic doubling route to chaos in a model of HIV infection of the immune system. *Simulation Practice and Theory*, 1(2):49–55, November 1993.

[26] R. A. Miranda. *Simulação numérica da interação onda-onda induzida por onda de Langmuir no sistema solar.* Dissertação de mestrado, Mestrado em Geofísica Espacial, Instituto Nacional de Pesquisas Espaciais, 2006.

[27] R. A. Miranda, E. L. Rempel, and A. C.-L. Chian. Chaotic saddles in nonlinear modulational interactions in a plasma. *Phys. Plasmas*, 19, November 2012.

[28] R. A. Miranda, E. L. Rempell, A. C.-L. Chian, N. Seehafer, B. A. Toledo, and P. R. Muñoz. Lagrangian coherent structures at the onset of hyperchaos in the two-dimensional Navier-Stokes equations. *Chaos*, 23(3), July 2013.

[29] T. Peacock and G. Haller. Lagrangian coherent structures: The hidden skeleton of fluid flows. *Phys. Today*, 66(2):41–46, February 2013.

[30] A. S. Perelson, D. E. Kirschner, and R. de Boer. Dynamics of HIV infection of CD4+ T cells. *Mathematical Biosciences*, 114(1):81–125, 1993.

[31] L. R. Petzold. Automatic selection of methods for solving stiff and non-stiff systems of ordinary differential equations. *SIAM J. Sci. and Stat. Comput*, 4(1):136–148, 1983.

[32] M. A. Savi. *Dinâmica Não-linear e Caos.* E-papers Serviços Editoriais, Rio de Janeiro, RJ, 1ª edition, 2006.

[33] A. B. Schelin, Gy. Károlyi, A. P. S. de Moura, N. A. Booth, and C. Grebogi. Chaotic advection in blood flow. *Phys. Rev. E*, 80(1):016213–1 – 016213–7, July 2009.

[34] S. C. Shadden, F. Lekien, and J. E. Marsden. Definition and properties of Lagrangian coherent structures from finite-time Lyapunov exponents in two-dimensional aperiodic flows. *Physica D: Nonlinear Phenomena*, 212(3–4):271–304, December 2005.

[35] S. H. Strogatz. *Nonlinear dynamics and chaos: with applications to physics, biology, chemistry, and engineering.* Perseus Books Publishing, L. L. C., New York, 1994.

[36] UNAIDS. *90–90–90 An ambitious treatment target to help end the AIDS epidemic.* Joint United Nations Programme on HIV/AIDS (UNAIDS), Geneva, Switzerland, 2014.

[37] UNAIDS. *Global HIV&AIDS statistics–2018 fact sheet.* Joint United Nations Programme on HIV/AIDS (UNAIDS), Geneva, Switzerland, 2019.

[38] S. S. Varghese, S. H. Frankel, and P. F. Fischer. Direct numerical simulation of stenotic flows, Part. 1 Steady flow. *J. Fluid Mech*, 582:253–280, July 2007.

[39] L. Wang. Global dynamical analysis of HIV models with treatments. *International Journal of Bifurcation and Chaos*, 22(9):1250227–1250238, September 2012.

[40] A. Wolf, J. B. Swift, H. L. Swinney, and J. A. Vastano. Determining Lyapunov exponents from a time series. *Physica D: Nonlinear Phenomena*, 16(3):285–317, July 1985.

A   APPENDIX

The equations of fluids solved by Comsol Multiphysics software are

$$\rho\frac{\partial u}{\partial t} + \rho\left(u \cdot \nabla\right)u = \nabla \cdot \left[-\rho I + \mu\left(\nabla u + (\nabla u)^T\right) - \frac{2}{3}\mu(\nabla \cdot u)I\right] + F$$

$$\frac{\partial \rho}{\partial t} + \nabla \cdot (\rho u) = 0$$

where ρ is the fluid density, $\vec{u}$ is the fluid velocity, μ is the dynamic viscosity, F is an external forcing term.

The blood flow is modelled in Comsol using the non-Newtonian Carneau model:

$$\mu = \mu_{inf} + (\mu_0 - \mu_{inf}) \cdot [1 + (\lambda \cdot \dot{y})^2]^{\frac{n-1}{2}}, \tag{A.1}$$

$$\dot{y} = max(\sqrt{D : D}, \dot{y}_{min}), D = \frac{1}{2} \cdot \nabla u + (\nabla u)^\tau], \tag{A.2}$$

where $\mu_0 = 0.161[Pa * s]$, $\mu_{inf} = 0.00345[Pa * s]$, $\lambda = 39.418s$,$n = 0.479l$. The μ_0 describes zero shear rate viscosity; μ_{inf} represents infinite shear rate viscosity; λ and n correspond to model parameters.